*J. Fluid Mech.* (2023), *vol*. 974, A46, doi:10.1017/jfm.2023.751

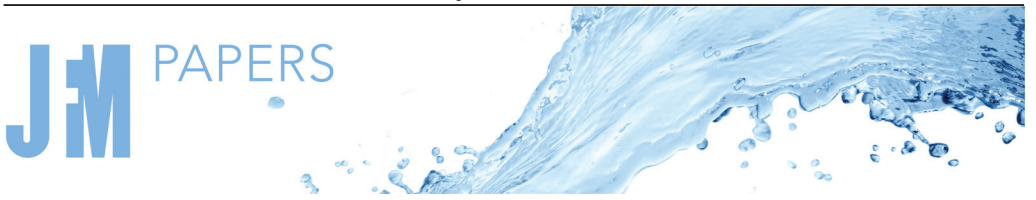

# One-dimensional mechanism of gaseous deflagration-to-detonation transition

**Paul Clavin**†

Aix Marseille Université, CNRS, Centrale Marseille, IRPHE UMR7342, 49 Rue F. Joliot Curie, 13384 Marseille, France

(Received 1 January 2023; revised 26 May 2023; accepted 5 September 2023)

A one-dimensional mechanism of deflagration to detonation transition is identified and investigated by an asymptotic analysis in the double limit of large activation energy and small Mach number of the laminar flame velocity. The unsteady analysis concerns the self-accelerating tip of an elongated flame in a smooth walled tube. The flame on the tip, considered as plane and orthogonal to the tube axis, is pushed from behind by the longitudinal flow resulting from the cumulative effect of the radial flows of burned gas issued from the lateral flame of the finger-like front (called backflow in the following). The analysis of the one-dimensional dynamics is performed by coupling the flame structure with the downstream-running compression waves propagating in the external flows. A critical elongation is identified from which the slightest increase in elongation leads to a pressure runaway producing the flame blow-off. The dynamics of the inner structure of the laminar flame on the tip which is accelerated by the self-induced backflow is characterized by a finite-time singularity of the reacting flow in the form of a dynamical saddle-node bifurcation.

**Key words:** detonation waves, bifurcation

## 1. Introduction

Deflagration-to-detonation transition (DDT) is observed in tubes filled with energetic gaseous mixtures such as stoichiometric hydrogen–oxygen or acetylene–oxygen mixtures. Deflagration-to-detonation transition is a fascinating phenomenon of abrupt transition (in less than a microsecond) between two opposite regimes of propagation, a markedly subsonic flame and a supersonic combustion wave. A detonation is a supersonic wave consisting in a smooth front of a strong inert shock followed by a thin reaction zone (including induction) across which viscosity, heat conduction and molecular diffusion of species are negligible. The overpressure is large, the pressure ratio ranging from 15 to 50. By comparison, each surface element of the brush of a turbulent flame is a quasi-isobaric

† Email address for correspondence: paul.clavin@univ-amu.fr

reaction–diffusion wave whose velocity relative to the gas (laminar flame velocity) is much smaller than the sound speed, typically by a factor $10^{-2}$. However, due to the increase in surface area of the wrinkled front, the speed of the flame brush (measured in the laboratory frame) becomes large, not far from the sound speed near the transition.

The pioneering experiments of Urtiew & Oppenheim (1966) have shown that the DDT onset is a local phenomenon occurring in a local explosion centre either on a surface element of the flame brush or in the viscous boundary layer ahead of the flame. We will not consider the latter case for which the DDT is more likely due to the gradient mechanism of Zeldovich (1980) reinforced by compressional heating, as discussed p. 260 in Clavin & Searby (2016) and observed in sub-millimetre tubes by the numerical simulation of Houim, Ozgen & Oran (2016). In the following, the attention is focused on the first case for which the explosion centre is on the flame outside the boundary layer. The origin and nature of the explosion centres remained unexplained. After more than a century of experimental works and decades of numerical studies, DDT is not yet understood, see Lee (2008) and Clavin & Searby (2016). Despite various attempts, there is no fundamental mechanism that is generally agreed upon as being universal. Neither the role of turbulence mentioned by Shchelkin & Troshin (1965) nor the gradient of induction time of Zeldovich (1980) are involved in the experiments and numerical simulations of Liberman *et al.* (2010), Kuznetsov, Liberman & Matsukov (2010) and Ivanov, Kiverin & Liberman (2011). These seminal works concern DDT of flames propagating in smooth walled tubes in which the induced flow of unburned gas is laminar in the bulk, the 3 mm boundary layer staying stuck at the wall near the flame, see p. 692 in Liberman *et al.* (2010). The detonation onset in these experiments is a local and sudden phenomenon occurring in a 'small explosion centre' on the flame front outside the boundary layer without any reflected shock (long tubes). Therefore the transition appears to be an intrinsic mechanism of a laminar flame accelerated by a self-induced flow. The DDT was also observed by Wu *et al.* (2007) and Wu & Wang (2011) in micro-scale tubes (0.5 mm radius) in which the transition concerns very elongated fronts of laminar flame. Kuznetsov *et al.* (2010), Ivanov *et al.* (2011) and Bykov *et al.* (2022) mentioned that the shocks formed in the immediate proximity ahead of the self-accelerating flame are suddenly overtaken by the reaction front. A striking observation is that the Mach number of these shocks is not larger than 2.5 so that the temperature of the compressed gas is not large enough for self-igniting the reactive mixture, ruling out the DDT mechanisms of Shchelkin & Troshin (1965) and of Zeldovich (1980).

A key mechanism underlying the DDT was identified long ago by Deshaies & Joulin (1989). Treating a turbulent flame brush as a planar discontinuity propagating at a subsonic velocity equal to the laminar flame velocity multiplied by a wrinkling factor $\sigma$, Deshaies & Joulin (1989) investigated the self-similar solutions characterized by a constant velocity of the weak shock ahead of the flame. They showed that, due to a laminar flame velocity highly sensitive to temperature changes, the self-similar solutions no longer exist above a critical value of $\sigma$ close to ten. The assumption of a weak shock used by Deshaies & Joulin (1989) can be easily removed without modifying qualitatively the result. The turning point of the curve 'self-similar solution vs $\sigma$' is due to a nonlinear thermal feedback loop: the laminar flame velocity is a function of the temperature which increases with the strength of the lead shock, the latter increasing in turn with the flame velocity. This pioneering analysis was overlooked by the combustion community during more than twenty years. A weaknesses of the self-similar solutions is the steady and uniform state of unburned-gas flow between the flame and the lead shock. A basic ingredient of the DDT is overlooked, namely the unsteady flow of the compression waves generated by the accelerating flame. The role of the flame acceleration has been invoked in the past

but with no connection to the turning point of Deshaies & Joulin (1989). However, in a series of articles starting nearly 10 years ago, Kagan & Sivashinsky (2017), motivated by the work of Deshaies & Joulin (1989), have investigated numerically the one-dimensional propagation of a laminar flame ignited at the closed end of a tube and sustained by a reaction rate which is increased artificially by a factor $\sigma^2$. For values of $\sigma$ above a critical value close to 10, namely close to the critical condition of Deshaies & Joulin (1989), the numerical results of Kagan & Sivashinsky (2017) show a sharp transition to detonation shortly after a quasi-isobaric ignition. An exothermic reaction rate which is a hundred times larger than the inelastic collision frequency of molecules associated with a large activation energy cannot describe real flames. Nevertheless, the numerical findings of Kagan & Sivashinsky (2017) are useful for improving our understanding of DDT: they suggest a runaway of the one-dimensional structure of 'fast' laminar flames, still markedly subsonic, resulting from the strong interaction near the turning point of Deshaies & Joulin (1989) between the acceleration-induced compression waves and the reaction–diffusion mechanisms sustaining a quasi-isobaric combustion wave.

The objective of the present paper is an attempt to describe theoretically such a one-dimensional DDT mechanism on the tip of a self-accelerating elongated flame using a combustion rate compatible with the kinetic theory of gas for a one-step Arrhenius law with a large activation energy. In order to enlighten the essential features, the problem will be over-simplified, keeping only the key mechanisms responsible for the spontaneous transition. The one-dimensional model is inspired by the schematic analysis of Clanet & Searby (1996) who treat the tip of the elongated front as a planar flame orthogonal to the tube axis while the side of the finger-like flame is quasi-parallel to the adiabatic tube wall. An essential ingredient for the DDT on the tip is the longitudinal backflow of burned gas generated by the cumulative effects of the combustion of the lateral side of the elongated flame front, see figure 1. This flow hits the flame on the tip from the burned-gas side with a flow velocity $u_b$ proportional to the flame elongation and also to the laminar flame velocity $U_b$. If the flame on the tip is treated as a discontinuity, the self-similar solutions present a turning point similar to that of Deshaies & Joulin (1989) for a turbulent wrinkled flame, the elongation of the finger front playing the role of the wrinkling factor $\sigma$. According to Clavin & Tofaili (2021), the critical condition is in good agreement with the DDT observed in the experiments of Liberman *et al.* (2010) and Kuznetsov *et al.* (2010). The backflow $u_b$ increasing with the elongation of the finger-like flame, the speed of the tip relative to the tube $U_P = u_b + U_b$ increases also. Therefore, the flame acting as a semi-transparent piston, compression waves are generated in the unburned gas. Still considering the flame as a discontinuity, the analysis has been recently extended beyond self-similarity to take into account the acceleration-induced transient flow in the unburned gas, see Clavin (2022) and Clavin & Champion (2022). A singularity of the flow gradient appears suddenly on the flame front when the elongation reaches the critical value while the velocity of the flame front, the pressure and the flame temperature remain finite. Even though no runaway of temperature and/or pressure is described by these preliminary analyses, the finite-time singularity of the flow gradient on the flame front suggests the existence of a fundamental DDT mechanism. In the present article, the analysis is further extended to the inner structure of the laminar flame by coupling the unsteady reaction–diffusion mechanisms controlling the flame structure to the downstream-running compression waves in the external flows. The solution demonstrates that a one-dimensional DDT mechanism exists in the form of a finite-time singularity of the reacting flow leading to blow off the inner structure of the laminar flame on the tip. More precisely, the singularity takes the form of a dynamical saddle-node bifurcation presented in classical textbooks

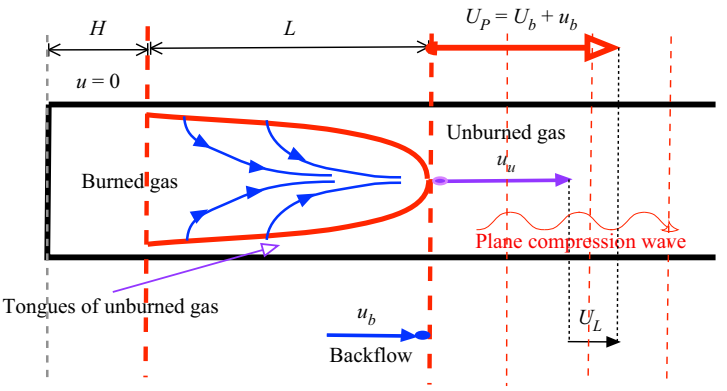


Figure 1. Sketch of the burned-gas flow in an elongated flame. The curved flame front propagating without deformation in a tube is characterized by $dL/dt \approx 0$ and $dH/dt \approx U_p$. The planar lead shock associated with the constant unburned-gas flow $u_u$ is far away from the flame tip. Downstream-running compression waves are launched in the unburned gas by the accelerating front as soon as the elongation increases so that the gas temperature is increased on the flame by adiabatic compression. Due to the nonlinear thermal feedback mentioned in the text, a drastic effect is produced at the critical flame velocity $U_P = U_P^*$ because the flame acceleration $dU_P/dt|_{U_P=U_P^*}$ diverges even when the elongation rate is small $dL/dt \ll U_p^*$. It is shown in this article that a finite-time singularity of the reacting flow occurs on the tip for $U_P(t)$ slightly larger than $U_p^*$.

of applied mathematics such as Binder & Orszag (1984) or Strogatz (1994). The key physical mechanism turns out to be the divergence of the flame acceleration that occurs systematically at the turning point for a small elongation rate as tiny as it may be. The turning point being associated with the nonlinear thermal feedback mentioned earlier, the critical condition has nothing to do with the Chapman–Jouguet (CJ) deflagration (sonic condition in the burned-gas flow) mentioned in the DDT literature for turbulent flames in tubes filled with obstacles. Such a sonic condition can never exist on the burned-gas side of laminar flames constituting the turbulent flame brush.

Unfortunately from a theoretical point of view, there is no satisfactory theory for the unsteady curved flow of burned gas sketched in figure 1. Hopefully a detailed analysis of the bunt gas flow is not needed for understanding the finite-time singularity. In the following, a small elongation rate is prescribed and a crude model for the unsteady backflow is used. In this context, an asymptotic analysis of the dynamics of the quasi-planar flame on the tip is then performed in the distinguished limit of large activation energy, small Mach number of the laminar flame and small elongation rate (smaller than the inverse of the transit time of fluid particles across the inner structure of the flame), the elongation having the same order of magnitude as the wrinkling factor in Deshaies & Joulin (1989). A similar analytical study can also be performed with a multiple-step chemical network representative of gaseous combustion if the production of the main radical is located in a thin reaction zone inside the inner flame structure, as it is usually the case. The essential point is the strong thermal sensitivity of the laminar flame velocity $(T/U_b)\, dU_b/dT \gg 1$ ($T$ is the temperature). Considering an elongated flame as a constitutive element of cellular flames, the DDT scenario could be relevant for wrinkled flames in tubes as well as for unstable flames expanding freely in open space.

The basic equations are recalled in § 2. The formulation of the problem in presented in § 3 where the backflow models are introduced. The asymptotic method is presented in § 4. Matching the quasi-isobaric flow in the flame structure (small length scale) with the external compressible flows is performed in § 5 where a general relation is obtained

linking the flow in an unsteady flame structure, the pressure and the flame temperature. The normal form of a dynamical saddle-node bifurcation describing the finite-time runaway of pressure and flame temperature is first derived in § 6 for a flame structure in steady state. A similar result is obtained in the more technical analysis of § 7 taking into account the unsteady inner structure of the laminar flame. Discussion and conclusion are presented in § 8.

## 2. The basic equations

A one-dimensional time-dependent combustion flow of an ideal gas is considered in a planar geometry with $x$ denoting the coordinate in the flow direction and $t$ the time. The propagation is from left to right.

### 2.1. *Conservative form*

The equations for mass and momentum are

$$\frac{\partial \rho}{\partial t} = -\frac{\partial(\rho u)}{\partial x}, \quad \frac{\partial(\rho u)}{\partial t} = -\frac{\partial\left[p + \rho u^2 - \mu \partial u \partial x\right]}{\partial x}, \tag{2.1a,b}$$

where $\rho$, $p$ and $u$ are respectively the density, the pressure and the velocity of the flow in the laboratory frame and $\mu$ is the viscosity. For the sake of simplicity we will consider an irreversible one-step exothermal reaction. This simplification can be removed and the fundamental result does not depend qualitatively on a detailed chemical scheme provided the laminar flame velocity is highly sensitive to the temperature. Introducing the progress variable $Y$, namely the mass fraction of products, $Y = 0$ in the unburned mixture and $Y = 1$ in the burned gas, the chemical heat release per unit mass $q_m$, the heat conductivity $\lambda$ and the diffusion coefficient $D$, the equation for energy, written in conservative form, is

$$\frac{\partial\left[\rho(c_v T + u^2/2 - q_m Y)\right]}{\partial t} = -\frac{\partial\left[\rho u\left(c_v T + p/\rho + u^2/2 - q_m Y\right) - \lambda \partial T/\partial x - \mu u \partial u/\partial x + q_m \rho D \partial Y/\partial x\right]}{\partial x}, \tag{2.2}$$

with the perfect gas law, $p = c_v(\gamma - 1)\rho T = n k_B T$ in which $k_B$ is the Boltzmann constant and $n$ the molecular density. The ratio of specific heats $\gamma \equiv c_p/c_v$ is assumed constant for simplicity. The conservation equation of species for a one-step reaction, written in terms of the progress variable, $Y \in [0, 1]$ reads

$$\frac{\partial(\rho Y)}{\partial t} = -\frac{\partial\left[\rho u Y - \rho D \partial Y/\partial x\right]}{\partial x} + \rho W(Y, T), \tag{2.3}$$

with a reaction rate in the form of an Arrhenius law for a large activation energy $\mathcal{E} \gg k_B T$, proportional to the frequency of binary collisions $1/t_{coll}$

$$W(Y, T) = \frac{B}{t_{coll}}(1 - Y)^2 \exp(-\mathcal{E}/k_B T). \tag{2.4}$$

These macroscopic equations are solutions of the Boltzmann equation in the hydrodynamic limit (macroscopic length scales larger than the mean free path and time larger than $t_{coll}$, respectively). The solution shows how the frequency of binary collisions

$1/t_{coll}$, the diffusion coefficient $D$ and the sound speed $a = \sqrt{\gamma p/\rho}$ are related in a perfect gas $p = nk_BT$

$$D = \frac{1}{6\sqrt{\gamma} n r_o^2} a, \quad \frac{D}{t_{coll}} = \frac{8\sqrt{\pi}}{3\gamma} a^2, \tag{2.5a,b}$$

$r_o$ being the radius of the molecules. The parameter $B$, usually called the pre-factor, is the reduced activation energy times the initial molecular dilution of reactant $y_i$

$$B = y_i \frac{\mathcal{E}}{k_BT} \quad \Rightarrow \quad B\frac{D}{t_{coll}} = \frac{8\sqrt{\pi}}{3} y_i \frac{\mathcal{E}}{m}. \tag{2.6}$$

Equations (2.5*a*,*b*) and (2.6) are useful to express the laminar flame velocity in terms of the flame temperature. For the sake of simplicity the molecules of reactants, products and diluent are assumed to have the same mass $m$ ($\rho = nm$) and the same radius $r_o$.

According to the asymptotic analysis of Zeldovich–Frank–Kamenetskii (ZFK), in the limit of large activation energy $\mathcal{E}/k_BT_b \gg 1$, the laminar flame velocity $U_b(T_b)$ relative to the burned gas denoted by the subscript $b$ ($T_b$ is the flame temperature) takes the form

$$U_b(T_b) = \frac{1}{\tilde{\beta}_b^{3/2}} \sqrt{8B_b \frac{D_b}{t_{collb}} \exp(-\mathcal{E}/k_BT_b)}, \quad \text{where } \tilde{\beta}_b \equiv \frac{q_m}{c_pT_b}\frac{\mathcal{E}}{k_BT_b}, \tag{2.7}$$

showing how small is the Mach number of the laminar flame velocity

$$\varepsilon \equiv \frac{U_b}{a_b} = \sqrt{\frac{2!\,16\pi^{1/2}}{3\gamma}} y_i \frac{1}{\tilde{\beta}_b^{3/2}} \sqrt{\frac{\mathcal{E}}{k_BT_b}} \exp(-\mathcal{E}/2k_BT_b); \tag{2.8}$$

see a didactic presentation in Clavin & Searby (2016). Typical orders of magnitude in real flames are $U_b/a_b \approx 10^{-3}$–$10^{-2}$. Equation (2.8) leads to similar values $\varepsilon \approx 10^{-3}$ for $\mathcal{E}/k_BT_b \approx 10$, $q_m/c_pT_b \approx 0.8$ and $\varepsilon \approx 10^{-2}$ for smaller values of $\mathcal{E}/k_BT_b$ in energetic mixtures. According to (2.5*a*,*b*)–(2.8), the ratio of the laminar flame velocity for two flames with different temperatures takes the form

$$\frac{U_b(T_{b1})}{U_b(T_{b2})} = \left(\frac{T_{b1}}{T_{b2}}\right)^3 \exp -\frac{\mathcal{E}}{2k_B}\left(\frac{1}{T_{b1}} - \frac{1}{T_{b2}}\right). \tag{2.9}$$

The main effect of a complex network of chemical kinetics is to modify the power law in the Arrhenius pre-factor and to introduce a temperature cutoff $T_c \in [850\text{–}1200\ \text{K}]$ below which the combustion cannot proceed. In addition, the activation energy $\mathcal{E}$ varies with the temperature for $T > T_c$. For a large activation energy $\mathcal{E}/(k_BT_b) \gg 1$ and far from the chemical quenching $T_b > T_c$, the temperature variation of $\mathcal{E}$ can be neglected in a limited range of flame temperature $\Delta T_b \ll \mathcal{E}/(\mathrm{d}\mathcal{E}/\mathrm{d}T_b)$. The upper bound of $\Delta T_b/T_b$ for the validity of this inequality is not small when the relative variation of the activation energy is smaller than the reduced activation energy $(T_b/\mathcal{E})\,\mathrm{d}\mathcal{E}/\mathrm{d}T_b < \mathcal{E}/k_BT_b$. In such conditions, (2.9) is reduced to an Arrhenius law

$$\beta \gg 1, \quad \frac{\mathcal{E}}{k_BT_{b2}}\left(\frac{T_{b1}}{T_{b2}} - 1\right) = O(1) : \ \frac{U_b(T_{b1})}{U_b(T_{b2})} \approx \exp\left[\frac{\mathcal{E}/2}{k_BT_{b2}}\left(\frac{T_{b1}}{T_{b2}} - 1\right)\right]. \tag{2.10}$$

However in highly reactive mixtures (stoichiometric $H_2$ or $C_2H_4$ mixtures in pure oxygen) the flame temperature is large and the reduced activation energy is of order unity so that the power law $(T_{b1}/T_{b2})^3$ in (2.9) cannot be ignored.

### 2.2. *Non-dimensional equations in the Lagrangian form*

From now on, the reference state used in the non-dimensional equations is the burned gas of the steady flame at the initial condition (labelled $i$). The latter is a self-similar solution with the lead shock at infinity. Denoting by $T_{ui}$ and $\rho_{bi}$ respectively the temperature of the unburned gas and the density of the burned gas in the initial state, the reference temperature, velocity, density and pressure are

$$T_{ref} = T_{bi} = T_{ui} + q_m/c_p, \quad U_{ref} = U_b(T_{bi}), \quad \rho_{ref} = \rho_{bi}, \quad p_{ref} = (c_p - c_v)\rho_{ref}T_{ref}. \tag{2.11a–d}$$

Using the corresponding flame thickness and transit time $d_{ref} = D_{ref}/U_{ref}$ and $t_{ref} = d_{ref}/U_{ref} = D_{ref}/U_{ref}^2$, where $D_{ref}$ is the molecular diffusion coefficient in the reference state, the following non-dimensional variables are introduced:

$$\tau \equiv t/t_{ref}, \quad \xi \equiv (x - X_P)/d_{ref}, \quad \text{where } t_{ref} \equiv d_{ref}/U_{ref} = D_{ref}/U_{ref}^2, \tag{2.12}$$

$$r \equiv \frac{\rho}{\rho_{ref}}, \quad v \equiv \frac{u}{U_{ref}}, \quad \pi \equiv \frac{p}{p_{ref}}, \quad \theta \equiv \frac{T}{T_{ref}}, \quad v_P \equiv \frac{U_P}{U_{ref}}, \tag{2.13a–e}$$

where $x = X_P(t)$ is the instantaneous position of the flame (for example, the maximum of reaction rate), $u(x, t)$ and $U_P(t) \equiv \mathrm{d}X_P/\mathrm{d}t$ are respectively the flow velocity and the propagation speed of the flame in the laboratory frame (not to be confused with the laminar flame velocity $U_b$). The non-dimensional mass flux across the flame $m \equiv \rho(U_P - u)/\rho_{ref}U_{ref}$ takes the form

$$m(\xi, \tau) = r\,[v_P(\tau) - v(\xi, \tau)] > 0, \quad r \equiv \pi/\theta. \tag{2.14}$$

Introducing the Mach number of the laminar flame, the reduced heat release and the reduced activation energy

$$\varepsilon \equiv \frac{U_{ref}}{a_{ref}} \approx 10^{-2}, \quad q \equiv \frac{q_m}{c_pT_{ref}} \approx 0.7, \quad \beta \equiv \frac{\mathcal{E}}{k_BT_{ref}} = 4\text{–}8, \tag{2.15a–c}$$

and using the relations $1/(\rho_{ref}c_pT_{ref}) = (\gamma - 1)/(\gamma p_{ref}) = (\gamma - 1)/(\rho_{ref}a_{ref}^2)$ and $D_{ref} = \lambda/(\rho_{ref}c_p) = \mu/\rho_{ref}$ ($Le = 1$ for simplicity), the non-dimensional Lagrangian form of (2.1*a*,*b*)–(2.4), written in the frame moving with the flame $t_{ref}\partial/\partial t \to \partial/\partial\tau - v_P\partial/\partial\xi$, reads

$$\frac{\partial r}{\partial \tau} = \frac{\partial m}{\partial \xi}, \quad r = \pi/\theta \tag{2.16}$$

$$\frac{\partial v}{\partial \tau} - m\frac{\partial v}{\partial \xi} = -\frac{1}{\gamma\varepsilon^2}\frac{\partial \pi}{\partial \xi} + \frac{\partial^2 v}{\partial \xi^2} \tag{2.17}$$

$$\left[r\frac{\partial}{\partial \tau} - m\frac{\partial}{\partial \xi}\right]Y - \frac{\partial^2 Y}{\partial \xi^2} = w(\theta, Y) \tag{2.18}$$

$$\left[r\frac{\partial}{\partial \tau} - m\frac{\partial}{\partial \xi}\right]\theta - \frac{(\gamma - 1)}{\gamma}\left[\frac{\partial}{\partial \tau} + [v - v_P]\frac{\partial}{\partial \xi}\right]\pi = \frac{\partial^2 \theta}{\partial \xi^2} + (\gamma - 1)\varepsilon^2\left(\frac{\partial v}{\partial \xi}\right)^2 + qw. \tag{2.19}$$

For a large activation energy, the non-dimensional reaction rate takes the form

$$w(\theta, Y) \equiv t_{ref} w = \frac{\beta_{ref}^3}{8} \frac{\pi_b}{\theta_b} (1-Y)^2 \exp\left[\frac{\mathcal{E}}{k_B T_{ref}} (\theta - 1)\right], \quad \beta_{ref} \equiv \frac{q_m}{c_p T_{ref}} \frac{\mathcal{E}}{k_B T_{ref}}, \tag{2.20a,b}$$

the subscript $b$ denoting the burned gas. Eliminating the density by using the perfect gas law $r = \pi/\theta$, the four equations (2.16)–(2.19) concern four fields $v(\xi, \tau)$, $\pi(\xi, \tau)$, $Y(\xi, \tau)$ and $\theta(\xi, \tau)$ plus an unknown function $v_P(\tau)$ appearing in the mass flux $m(\xi, \tau)$ (2.14).

### 2.3. *Mass-weighted coordinate*

The analysis of the unsteady flame structure is more easily performed using the mass-weighted coordinate $z$ and the reduced mass flux at the origin ($z = 0$) $m(\tau) \equiv m(z = 0, \tau)$ with, according to (2.14)

$$m(\tau) = r(0, \tau)\,[v_P(\tau) - v(0, \tau)] = \frac{\pi(0, \tau)}{\theta(0, \tau)}\,[v_P(\tau) - v(0, \tau)] > 0. \tag{2.21}$$

Introducing the change of variables $(\xi, \tau) \to (z, \tau)$

$$z \equiv \int_0^\xi r(\xi', \tau)\, \mathrm{d}\xi', \quad \frac{\partial}{\partial \xi} = r \frac{\partial}{\partial z} = \frac{\pi}{\theta} \frac{\partial}{\partial z}, \tag{2.22a,b}$$

$$\left.\frac{\partial}{\partial \tau}\right|_\xi = \left.\frac{\partial}{\partial \tau}\right|_z + \left[\int_0^\xi \frac{\partial r(\xi', \tau)}{\partial \tau} \mathrm{d}\xi'\right] \frac{\partial}{\partial z} = \left.\frac{\partial}{\partial \tau}\right|_z + [m(\xi, \tau) - m(\tau)] \frac{\partial}{\partial z}, \tag{2.23}$$

$$(v - v_P(\tau)) \frac{\partial}{\partial \xi} = -m(\xi, \tau) \frac{\partial}{\partial z} \Rightarrow \left.\frac{\partial}{\partial \tau}\right|_\xi + (v - v_P(\tau)) \frac{\partial}{\partial \xi} = \left.\frac{\partial}{\partial \tau}\right|_z - m(\tau) \frac{\partial}{\partial z}, \tag{2.24}$$

where the function $m(\tau)$ in front of the derivative with respect to $z$ depends only on the time. Continuity (2.16) written with the variables $(z, \tau)$

$$r \frac{\partial m(z, \tau)}{\partial z} = \frac{\partial r(z, \tau)}{\partial \tau} + [m(z, \tau) - m(\tau)] \frac{\partial r}{\partial z}, \tag{2.25}$$

yields after multiplication by $1/r^2$

$$\frac{1}{r} \frac{\partial m(z, \tau)}{\partial z} = -\left.\frac{\partial (1/r)}{\partial \tau}\right|_z - [m(z, \tau) - m(\tau)] \frac{\partial (1/r)}{\partial z}, \tag{2.26}$$

to give, using (2.14) $m(z, \tau) = -r(z, \tau)[v(z, \tau) - v_P(\tau)] > 0$,

$$\frac{\partial m(z, \tau)}{\partial z} = -[v(z, \tau) - v_P(\tau)] \frac{\partial r}{\partial z} - r \frac{\partial v}{\partial z} \quad \Rightarrow \quad \frac{\partial v}{\partial z} = \left.\frac{\partial (1/r)}{\partial \tau}\right|_z - m(\tau) \frac{\partial (1/r)}{\partial z}, \tag{2.27}$$

yielding the gradient of the flow in terms of $1/r = \theta(z, \tau)/\pi(z, \tau)$. For simplicity, the diffusion coefficient $D$ is assumed to verify $\rho^2 D =$ constant, $\partial(\rho D \partial/\partial x)/\partial x \to$

$(\rho^2 D/\rho_{ref}^2 D_{ref}) r\partial^2/\partial z^2 = r\partial^2/\partial z^2$. Then, (2.16)–(2.19) yield

$$\frac{\partial v}{\partial z} = \left[\frac{\partial}{\partial \tau} - m(\tau)\frac{\partial}{\partial z}\right]\frac{\theta}{\pi},$$

$$= \frac{1}{\pi}\left[\frac{\partial}{\partial \tau} - m(\tau)\frac{\partial}{\partial z}\right]\theta - \frac{\theta}{\pi^2}\left[\frac{\partial}{\partial \tau} - m(\tau)\frac{\partial}{\partial z}\right]\pi \tag{2.28}$$

$$\left[\frac{\partial v}{\partial \tau} - m(\tau)\frac{\partial v}{\partial z} - \frac{\partial^2 v}{\partial z^2}\right] = -\frac{1}{\gamma \varepsilon^2}\frac{\partial \pi}{\partial z} \tag{2.29}$$

$$\left[\frac{\partial Y}{\partial \tau} - m(\tau)\frac{\partial Y}{\partial z} - \frac{\partial^2 Y}{\partial z^2}\right] = w(\theta, Y), \quad Y(z, \tau) \in [0, 1] \tag{2.30}$$

$$\left[\frac{\partial \theta}{\partial \tau} - m(\tau)\frac{\partial \theta}{\partial z} - \frac{\partial^2 \theta}{\partial z^2}\right] = qw(\theta, Y) + \frac{(\gamma - 1)}{\gamma}\frac{\theta}{\pi}\left[\frac{\partial \pi}{\partial \tau} - m(\tau)\frac{\partial \pi}{\partial z}\right] + (\gamma - 1)\varepsilon^2\left(\frac{\partial v}{\partial z}\right)^2, \tag{2.31}$$

where the perfect gas law $r = \pi/\theta$ has been used to eliminate the density. When the dissipative terms (heat conduction, viscosity and reaction rate) are neglected, equation for energy (2.31) takes the form of the entropy wave in an inert gas

$$\frac{1}{\theta}\left[\frac{\partial \theta}{\partial \tau} - m(\tau)\frac{\partial \theta}{\partial z}\right] - \frac{(\gamma - 1)}{\gamma}\frac{1}{\pi}\left[\frac{\partial \pi}{\partial \tau} - m(\tau)\frac{\partial \pi}{\partial z}\right] = 0. \tag{2.32}$$

## 3. Formulation of the problem

Ignited at the closed end of a smooth walled tube, a laminar flame takes an elongated shape with a curved flow of burned gas striking the flame on the tip from behind (backflow) sketched in figure 1. The attention is focused soon after the formation of the tulip flame when the finger shaped flame front is recovered and evolves slowly. Two basic mechanisms are involved in the DDT on the tip of the elongated flame: firstly the increase of the backflow of burned gas on the tip $u_b(t)$ with both the elongation and the laminar flame velocity, and secondly the increase of the laminar flame velocity with the flame temperature. In the following, the elongation of the finger flame $S(\tau)$ is a given increasing function of the time $\mathrm{d}S(\tau)/\mathrm{d}\tau > 0$ starting at $\tau = 0$ from a self-similar solution whose elongation is $S_i \equiv S(0) \geqslant 1$. The increase rate is assumed smaller than the inverse of the transit time of a fluid particle across the flame structure

$$S(\tau) = [1 + \epsilon\tau]S_i, \quad \text{with } \varepsilon \ll \epsilon \ll 1. \tag{3.1}$$

The relation $\varepsilon \ll \epsilon$ is useful to take into account unsteady effects while neglecting the terms of order $\varepsilon^2$. As we shall see, a finite-time singularity of the flow is predicted for any $\epsilon > 0$, as small it can be. Under the condition (3.1), the curvature of the flame is negligible and the compression waves are quasi-planar if the tube radius $R$ is in the range $\varepsilon(R/d) = O(1)$.

### 3.1. *Backflow models*

The flame on the tip is treated as planar and orthogonal to the propagation axis. Following Clanet & Searby (1996), the longitudinal gradient of burned-gas flow on the tube axis

$u(x,t)$ is roughly modelled by a source term of mass whose origin is the burning of the lateral flame parallel to the wall. Denoting the laminar flame velocity (relative to the burned gas) of this lateral flame $U_{bw}(x,t)$, the gradient of the flow on the tube axis $u(x,t)$ is approximated by a one-dimensional mass conservation in an incompressible flow

$$\frac{\partial u}{\partial x} = \frac{2}{R} U_{bw}(x,t), \tag{3.2}$$

where $R$ is the radius of the tube. The longitudinal backflow $u_b(t)$ impinging the tip from behind is obtained by integration along the axis of the finger flame. For a closed-end tube on the burned-gas side, assuming that the incompressible flow of burned gas is at rest behind the elongated flame, one gets

$$u_b(t) \equiv u(x = X_p(t), t) = \frac{2}{R} \int_{X_P - L}^{X_P} U_{bw}(x,t)\, \mathrm{d}\, x, \tag{3.3}$$

where $X_p(t)$ is the position of the tip and $L(t)$ the length of the elongated flame. Neglecting both the heat loss on the wall and the unsteadiness of the burned-gas flow treated as incompressible, $U_{bw}$ is uniform along the lateral flame and equal to the laminar flame speed on the tip at the same time $U_{bw} = U_b(t)$. Moreover, if the unsteadiness of the inner flame structure is negligible, $U_b(t)$ is given by (2.7)–(2.10) $U_b(t) = U_b(T_b(t))$. Under these approximations, the backflow takes the form introduced by Clavin & Tofaili (2021)

$$\text{instantaneous backflow model:} \quad u_b(t) = S(t)\, U_b(t), \quad U_b(t) \equiv U_b\left(T_b(t)\right), \tag{3.4}$$

where $S$ is the elongation of the finger flame ($S = 2L/R$ in cylindrical geometry) and $T_b(t) = T_u(t) + Q/c_p$ where $T_u(t)$ is the temperature of the fresh mixture just ahead of the flame.

Unsteadiness of the flow of burned gas in an elongated flame is too complicated to be described analytically. Hopefully a detailed study is not useful in the following. This unsteady effect will be roughly modelled by a delay $\Delta t(X_P - x)$ for transferring to the tip the flow of burned gas issued from the lateral flame at a distance $X_p - x$ from the tip

$$u_b(t) \approx \frac{2}{R} \int_{X_P - L}^{X_P} U_b\left(t - \Delta t(X_P - x)\right) \mathrm{d}\, x. \tag{3.5}$$

Assuming a slow evolution of the laminar flame velocity $U_b/(\mathrm{d}U_b/\mathrm{d}t) \gg \Delta t(L) \geqslant \Delta t(X_P - x)$, a Taylor expansion yields

$$u_b(t) \approx \frac{2L(t)}{R} U_b(t) - \frac{2}{R} \frac{\mathrm{d}U_b}{\mathrm{d}t} \int_{X_P - L}^{X_P} \Delta t(X_P - x)\, \mathrm{d}\, x. \tag{3.6}$$

Assuming that the variation of the radial burned gas out of the lateral flames is propagated by the downstream-running compression waves with a quasi-constant sound speed $a$, $\Delta t(X_P - x) \approx (X_P - x)/a$,

$$\int_{X_P - L}^{X_P} \Delta t(X_P - x)\, \mathrm{d}\, x \approx L^2/2a, \tag{3.7}$$

equation (3.6) yields, after introducing the overall delay $\Delta t_w \approx (1/2)L/a$,

$$\text{delayed model of backflow:} \quad u_b(t) \approx S(t) \left[ U_b(t) - \Delta t_w \frac{\mathrm{d}U_b}{\mathrm{d}t} \right] \approx S(t)\, U_b(t - \Delta t_w), \tag{3.8}$$

in which the variation with the time of $\Delta t_w$ is a negligible second-order effect.

### 3.2. *Limit of large activation energy*

The ZFK analysis in the limit of large activation energy has been extended more than forty years ago to unsteady structure of flames, see Clavin & Searby (2016) for a didactic presentation. Choosing the instantaneous position of the reaction sheet as the origin on the $z$-axis and introducing the notation

$$\beta \equiv \mathcal{E}/k_B T_{ref}, \quad \theta_b(\tau) \equiv T_b(t)/T_{ref}, \tag{3.9a,b}$$

for the reduced activation energy and the reduced flame temperature, the jump conditions on the reaction sheet take the form

$$\left.\begin{aligned} z \leqslant 0: \quad & Y = 1, \\ z = 0: \quad Y = 1, \quad & \theta = \theta_b(\tau), \quad (\theta_b - 1) = O(1/\beta), \end{aligned}\right\} \tag{3.10}$$

$$\beta \gg 1, \quad \beta(\theta_b - 1) = O(1): \quad \left.\frac{\partial \theta}{\partial z}\right|_{z=0^+} = -q \exp\left[\frac{\beta}{2}(\theta_b - 1)\right] + O(1/\beta), \tag{3.11}$$

$$\left.\frac{\partial \theta}{\partial z}\right|_{z=0^-} = \left.\frac{\partial \theta}{\partial z}\right|_{z=0^+} - q \left.\frac{\partial Y}{\partial z}\right|_{z=0^+} + O(1/\beta^2), \tag{3.12}$$

with $z = 0^+$ and $z = 0^-$ denoting the preheated zone side of the reaction zone and the exit on the burned-gas side, respectively. Equation (3.11) is valid to order unity while (3.12) is valid up to first order $1/\beta \ll 1$ (included). The backflow of burned gas is applied on the reaction sheet so that a boundary condition concerning the flow velocity is added

$$z = 0 \quad \tau > 0: \quad v = v_b(\tau), \tag{3.13}$$

$$\tau \leqslant 0: \quad v = v_b(0) = S_i. \tag{3.14}$$

To leading order in the limit $\beta \gg 1$, the variation of flame temperature is retained in the Arrhenius factor of (2.10) only. Therefore, when the inner flame structure is in steady state (denoted by an overbar), the laminar flame velocity reads

$$\beta \gg 1, \quad \beta(\bar{\theta}_b - 1) = O(1): \ \bar{U}_b(T_b)/U_{ref} = \bar{m} = \exp\left[\beta\left(\bar{\theta}_b - 1\right)/2\right] + O(1/\beta), \tag{3.15}$$

where $\bar{\theta}_b(\tau) = \theta_u(\tau) + q$ is the flame temperature and $\theta_u(\tau) = T_u(\tau)/T_{ref}$ the instantaneous temperature of unburned gas just ahead of the flame. The instantaneous backflow (3.4), written in non-dimensional form, then yields

$$\bar{v}_b(\tau) = S(\tau)\bar{m} = [1 + \epsilon\tau] S_i \exp\left(\beta\left[\theta_u(\tau) + q - 1\right]/2\right), \tag{3.16}$$

and the delayed backflow model (3.8) reads

$$\beta \gg 1, \quad \tau \geqslant 0: \quad v_b(\tau) = \bar{v}_b(\tau)\left[1 - (\beta/2)\frac{\Delta t_w}{t_{ref}}\frac{\mathrm{d}\theta_u}{\mathrm{d}\tau}\right], \quad \Delta t_w \approx \frac{L}{2a}. \tag{3.17a–c}$$

When the unsteadiness of the inner structure of the flame (studied in § 7) is taken into account, the mass flux $\bar{m}$ in (3.17*a–c*) is replaced by its unsteady version $m(\tau) = \bar{m} + \delta m$, $\bar{v}_b = S(\tau)\bar{m} \to S(\tau)m(\tau)$, the reduced backflow including the two unsteady effects (in the burned gas and in the inner flame structure) takes the form,

$$\beta \gg 1, \ \tau \geqslant 0: \ v_b(\tau) = S(\tau)\exp(\beta[\bar{\theta}_b(\tau) - 1]/2)\left[1 + \frac{\delta m(\tau)}{\bar{m}(\tau)}\right]\left[1 - (\beta/2)\frac{\Delta t_w}{t_{ref}}\frac{\mathrm{d}\theta_u}{\mathrm{d}\tau}\right]. \tag{3.18a,b}$$

Here, $\delta m(\tau)$ is computed by the unsteady analysis of the inner structure.

### 3.3. *Initial condition*

Before the elongation starts to increase, the initial condition is a self-similar solution (constant elongation, steady flame structure, $\theta_b(0) = 1$) with a constant backflow (3.14) $v_b(0) = S_i$ and a uniform flow ahead of the flame $\theta = 1 - q$, $v = v_b(0) + q$, the lead shock far ahead from the flame front being considered at infinity. The problem being hyperbolic in the unburned gas outside the flame structure, the downstream boundary condition far away from the flame for solving the unsteady problem is given by the initial solution

$$\left.\begin{array}{c} z \to \infty : \quad \pi \approx 1 + O(\varepsilon^2), \quad Y = 0, \quad \theta = 1 - q + O(\varepsilon^2), \\ v = S_i + q + O(\varepsilon^2). \end{array}\right\} \tag{3.19}$$

The neglected terms are of the same order of magnitude as the pressure jump across a laminar flame $\delta p/p = O(\varepsilon^2)$, according to the steady-state version of (2.29).

## 4. Asymptotic method

The problem is solved in the double limit of large activation energy $\beta \gg 1$ and small Mach number of the laminar flame $\varepsilon \ll 1$. A first quick look to the compressible flow of unburned gas ahead of the accelerating flame enlightens the multiple length-scale problem.

### 4.1. *Preliminary insights into the unburned-gas flow ahead of the flame*

When the flame accelerates the flame acts a semi-transparent piston so that simple compression waves are sent in the unburned gas. The dissipative mechanisms being negligible in this external flow, the entropy wave (2.32) propagates from right to left in the reference frame attached to the flame since the flame runs from left to right faster than the flow in the laboratory flame, $m(\tau) > 0$. Therefore, as long as no new shock wave is formed on the leading edge of the compression wave, the entropy is constant ahead of the flame and equal to the downstream entropy ($z \to \infty$). The isentropic condition $\pi = \theta^{\gamma/(\gamma-1)}$ for small pressure variations, $\theta = \theta_i(z) + \delta\theta$, $\pi = 1 + \delta\pi$, $\lim_{z\to\infty} \theta_i = 1 - q$, yields

$$\delta\pi \ll 1 : \quad \delta\theta/\theta_i(z) = [(\gamma - 1)/\gamma]\delta\pi, \tag{4.1}$$

the subscript $i$ denoting the initial unperturbed flow $\tau = 0 : \pi_i = 1$. Anyway, in the limit of small Mach number of the laminar flame $\varepsilon \ll 1$, the shocks that could be produced by the accelerating flame are weak so that the small entropy jump across the shock is of order of magnitude $\varepsilon^3$ and thus is negligible when the analysis is limited to $\varepsilon$-term. Then, according to continuity, (2.28),

$$\delta\pi = O(\varepsilon), \quad z \gg 1 : \frac{\partial v}{\partial z} = \left[\frac{\partial}{\partial \tau} - m(\tau)\frac{\partial}{\partial z}\right][\delta\theta - \theta_i\delta\pi] = -\theta_i\frac{1}{\gamma}\left[\frac{\partial}{\partial \tau} - m(\tau)\frac{\partial}{\partial z}\right]\delta\pi. \tag{4.2a,b}$$

The viscosity being negligible ahead of the flame, (2.29) yields

$$\delta\pi \ll 1 : \quad \left[\frac{\partial}{\partial \tau} - m(\tau)\frac{\partial}{\partial z}\right] v = -\frac{1}{\gamma\varepsilon^2}\frac{\partial \delta\pi}{\partial z}. \tag{4.3}$$

The flow $v(z, \tau)$ can be eliminated from (4.2a,b) and (4.3) to give in the linear approximation

$$\frac{(1-q)}{\pi^2}\left[\frac{\partial}{\partial \tau} - m(\tau)\frac{\partial}{\partial z}\right]^2 \delta\pi = \frac{1}{\varepsilon^2}\frac{\partial^2}{\partial z^2}\delta\pi. \tag{4.4}$$

Therefore, considering a time scale of the order of the transit time of fluid particles across the flame, $\partial/\partial\tau = O(1)$, the pressure varies in space with a length scale larger than the flame thickness by a factor of order $1/\varepsilon$

$$\frac{\partial\delta\pi/\partial z}{\partial\delta\pi/\partial\tau} = O(\varepsilon). \tag{4.5}$$

The unsteady term of (4.4) balances the second derivative with respect to space on the right-hand side since the term $[m\partial\pi/\partial z]$ is negligible in front of $[(1/\varepsilon)\partial\pi/\partial z]$ for $m = O(1)$. Therefore, the pressure fluctuation satisfies the linear wave equation

$$\varepsilon \ll 1: \quad \frac{\partial^2\delta\pi}{\partial\tau^2} = \frac{(1-q)}{\varepsilon^2}\frac{\partial^2\delta\pi}{\partial z^2}; \quad a^2 = \theta a_{ref}^2 \Rightarrow \frac{\partial^2\delta\pi}{\partial t^2} \approx a_i^2\frac{\partial^2\delta\pi}{\partial x^2}, \tag{4.6a,b}$$

written in the original variables using (2.12) and (2.22*a*,*b*). Therefore, in the limit $\varepsilon \ll 1$, the external flow of unburned gas ahead of the flame is governed by the linear acoustics with a negligible Doppler effect $m(\partial\delta\pi/\partial z)/(\partial\delta\pi/\partial\tau) = O(\varepsilon)$ leading to the scalings

$$\tau = O(1) \quad \Rightarrow \quad \varepsilon z = O(1). \tag{4.7}$$

According to the continuity equation (4.2*a*,*b*), $\partial v/\partial z$ is of order $\partial\delta\pi/\partial\tau$. Anticipating that the change in flow velocity is of order $S_i$ times the laminar flame velocity $\delta v = O(S_i)$, $\delta v$ and the pressure vary on the large length scale $\partial v/\partial z = O(\varepsilon S_i)$, the variation of the non-dimensional pressure $\delta\pi$ in the external zone is of order $\varepsilon S_i$. In the external zone ahead of the flame, the pressure takes the form

$$\pi = 1 + \varepsilon\pi_1(\varepsilon z, \tau), \quad \pi_1 = O(S_i). \tag{4.8a,b}$$

The nonlinear solution of the compression wave obtained by Clavin & Champion (2022) confirms that the limit $\varepsilon \ll 1$ leads to the linear wave (4.6*a*,*b*)–(4.8*a*,*b*).

### 4.2. *Distinguished limit*

According to (4.8*a*,*b*), the spatial variation of pressure in the external flow $\delta\pi = \varepsilon\pi_1 = O(\varepsilon S_i)$, is larger than in the inner structure of the flame by a factor $1/\varepsilon$ since $\pi_u - \pi_b = \gamma\varepsilon^2(v_u - v_b)\,m$ where the subscript $u$ denotes the unburned state just ahead of the flame. Neglecting terms of order $\varepsilon^2$, the pressure is treated as uniform inside the preheated zone of the flame structure $z = O(1) : 1 - \pi = O(\varepsilon^2)$. This is also the case in the thin reaction zone $z = O(1/\beta)$ across which the gradient of the flow velocity varies of order unity so that, according to (2.29), $\partial^2 v/\partial z^2 \approx (\partial\pi/\partial z)/\gamma\varepsilon^2 \Rightarrow \partial v/\partial z|_{0-}^{0+} \approx \pi|_{0-}^{0+}/\gamma\varepsilon^2 = O(1) \Rightarrow \pi|_{0-}^{0+} = O(\varepsilon^2)$. According to (3.15) in the limit of large activation energy $\beta \gg 1$, the compressional heating (4.1) influences the laminar flame velocity and the flame structure as soon as the compression-induced increase of the flame temperature is of the same order of magnitude as the inverse of the activation energy $(\gamma - 1)\,\delta\pi = O(1/\beta) \Rightarrow (\gamma - 1)\,\varepsilon\delta S_i = O(1/\beta)$. Therefore, as in the previous analysis of Clavin (2022), the distinguished limit to be considered in the DDT study is similar to that in Deshaies & Joulin (1989)

$$\varepsilon \to 0, \quad \beta \to \infty: \quad (\gamma - 1)\,\beta\varepsilon\,S_i = O(1). \tag{4.9}$$

The comparison with the ZFK expression (2.8) of $\varepsilon$ yields the order of magnitude of $S_i$, typically between 5 and 10.

### 4.3. *Equations in the limit* $\varepsilon \ll 1$

According to (4.8*a*,*b*), the pressure disturbance is small and varies in space on the rescaled coordinate $z_1 \equiv \varepsilon z = O(1)$

$$\partial\pi/\partial z = O(\varepsilon^2 S_i), \quad \pi = 1 + \varepsilon\pi_1(z_1, \tau), \quad \pi_1 = O(S_i), \quad z_1 \equiv \varepsilon z. \tag{4.10a–d}$$

Outside the thin reaction sheet, neglecting second-order terms $O(\varepsilon^2)$, (2.28)–(2.31) take the form

$$\left.\begin{aligned} \pi = 1 + \varepsilon\pi_1: \quad & \frac{\partial v}{\partial z} = \left[\frac{\partial}{\partial \tau} - m(\tau)\frac{\partial}{\partial z}\right]\frac{\theta}{1+\varepsilon\pi_1}, \\ \varepsilon \ll 1: \quad & \frac{\partial v}{\partial z} = [1-\varepsilon\pi_1]\left[\frac{\partial}{\partial \tau} - m(\tau)\frac{\partial}{\partial z}\right]\theta - \varepsilon\theta\left[\frac{\partial \pi_1}{\partial \tau} - m(\tau)\frac{\partial \pi_1}{\partial z}\right] + O(\varepsilon^2), \end{aligned}\right\} \tag{4.11}$$

$$\left[\frac{\partial v}{\partial \tau} - m(\tau)\frac{\partial v}{\partial z} - \frac{\partial^2 v}{\partial z^2}\right] = -\frac{1}{\gamma}\frac{1}{\varepsilon}\frac{\partial \pi_1}{\partial z} \tag{4.12}$$

$$\left[\frac{\partial Y}{\partial \tau} - m(\tau)\frac{\partial Y}{\partial z} - \frac{\partial^2 Y}{\partial z^2}\right] = 0, \quad Y(z,\tau) \in [0,1] \tag{4.13}$$

$$\left[\frac{\partial \theta}{\partial \tau} - m(\tau)\frac{\partial \theta}{\partial z} - \frac{\partial^2 \theta}{\partial z^2}\right] = \varepsilon\frac{(\gamma-1)}{\gamma}\theta\left[\frac{\partial \pi_1}{\partial \tau} - m(\tau)\frac{\partial \pi_1}{\partial z}\right] + O(\varepsilon^2). \tag{4.14}$$

Equation (4.14) shows how the effect of compressional heating in the unburned gas outside the flame thickness ($z \gg 1$: $[1/\theta]\partial\theta/\partial\tau = \varepsilon[(\gamma-1)/\gamma]\partial\pi_1/\partial\tau$) is transmitted to the reaction sheet ($z = 0$) by the entropy wave, as it is modified by the heat conduction inside the preheated zone (second derivative on the left-hand side). According to (4.10*a–d*), the terms involving $\partial\pi_1/\partial z = O(\varepsilon)$ in (4.11) and (4.14) are negligible in the inner structure of the flame (of order $\varepsilon^2$)

$$\frac{\partial v}{\partial z} = [1-\varepsilon\pi_1]\left[\frac{\partial}{\partial \tau} - m(\tau)\frac{\partial}{\partial z}\right]\theta - \varepsilon\theta\frac{\partial \pi_1}{\partial \tau} + O(\varepsilon^2), \tag{4.15}$$

$$\left[\frac{\partial \theta}{\partial \tau} - m(\tau)\frac{\partial \theta}{\partial z} - \frac{\partial^2 \theta}{\partial z^2}\right] = \varepsilon\frac{(\gamma-1)}{\gamma}\theta\frac{\partial \pi_1}{\partial \tau} + O(\varepsilon^2). \tag{4.16}$$

Introducing (4.16) into (4.15), the flow gradient inside the flame structure is expressed in terms of the heat flux and the time derivative of the pressure

$$\frac{\partial v}{\partial z} = [1-\varepsilon\pi_1]\frac{\partial^2 \theta}{\partial z^2} - \varepsilon\frac{1}{\gamma}\theta\frac{\partial \pi_1}{\partial \tau} + O(\varepsilon^2). \tag{4.17}$$

To summarize, in the distinguished limit (4.9), the problem consists in solving (4.12), (4.13), (4.16) and (4.17) with the jump conditions (3.10)–(3.16) on the reaction sheet and the boundary conditions (3.19) at infinity.

Here the problem is solved analytically in the frame attached to the reaction sheet by an asymptotic method. The corresponding one-dimensional numerical analysis to be performed later for the purpose of comparison is not straightforward. Solving the basic equations for a reaction rate given $W(Y, T)$ as an initial value problem would require to apply a boundary condition at the exit of the moving reaction zone, which is not so usual, see the text below (7.16).

## 5. Matching conditions. Flow in the unsteady flame structure

### 5.1. *Back to the external flow ahead of the flame*

Denoting the external flow ahead of the flame by the subscript $ext_+$ the initial condition takes the form

$$\tau = 0: \quad \theta_{ext_+} = 1 - q, \quad v_{ext_+} = S_i + q, \quad \pi = 1, \quad (\pi_1 = 0). \tag{5.1a–d}$$

Using the rescaled coordinate $z_1 = \varepsilon z$ in (4.10*a–d*), (4.1) and (4.8*a*,*b*)

$$\theta_{ext_+}(z_1, \tau) = (1 - q)\left[1 + \varepsilon\frac{\gamma - 1}{\gamma}\pi_1(z_1, \tau)\right] + O(\varepsilon^2), \tag{5.2}$$

equation (4.17) takes the form

$$\left.\begin{gathered}\frac{\partial v_{ext_+}}{\partial z} = [1 - \varepsilon\pi_1]\left[\frac{\partial}{\partial\tau} - m(\tau)\frac{\partial}{\partial z}\right]\theta_{ext_+} - \varepsilon\theta_{ext_+}\frac{\partial\pi_1}{\partial\tau} + O(\varepsilon^2) \\ \text{yielding} \quad \frac{\partial v_{ext_+}(z_1, \tau)}{\partial z_1} = -(1 - q)\frac{1}{\gamma}\frac{\partial\pi_1(z_1, \tau)}{\partial\tau} + O(\varepsilon)\end{gathered}\right\}. \tag{5.3}$$

Combined with the leading order of (4.12) in the external flow

$$\frac{\partial v_{ext_+}(z, \tau)}{\partial\tau} = -\frac{1}{\gamma}\frac{\partial\pi_1(z_1, \tau)}{\partial z_1} + O(\varepsilon), \tag{5.4}$$

the derivative of (5.3) with respect to $\tau$, after elimination of $v_{ext_+}$, leads to the wave equation (4.6*a*,*b*) for the pressure

$$\varepsilon \ll 1: \quad \frac{\partial^2\pi_1(z_1, \tau)}{\partial\tau^2} = \frac{1}{1 - q}\frac{\partial^2\pi_1(z_1, \tau)}{\partial z_1^2} + O(\varepsilon), \tag{5.5}$$

where, in the mass-weighted coordinates, the non-dimensional sound speed in the external zone is $1/\sqrt{1 - q}$. This is easily confirmed as follows:

$$z_1 = \varepsilon z = [U_{ref}/a_{ref}][\rho/\rho_{ref}]x/[U_{ref}t_{ref}], \tag{5.6}$$

using $\tau = t/t_{ref}$, the ratio $z_1/\tau$ takes the form $z_1/\tau = [x/at]\rho a/[\rho_{ref}a_{ref}]$ to give, using $\rho a/[\rho_{ref}a_{ref}] = [p/p_{ref}]\sqrt{T_{ref}/T}$, $(z_1/\tau) = [(x/at)/\sqrt{\theta}][1 + O(\varepsilon)]$ with, according to (5.2), $\theta = 1 - q + O(\varepsilon)$.

The flow of unburned gas being uniform and steady far ahead from the flame, the external flow is a downstream-running compression wave (propagating in the same direction as the flame) with a leading edge in the form of a weak singularity propagating with the sound speed relative to the flow. Then, according to (5.5), $\pi_1(z_1, \tau)$ and $v_{ext_+}(z_1, \tau) = S_i + q + \delta v_{ext_+}(z_1, \tau)$ are functions of a single variable $\tau - \sqrt{1 - q}\,z_1$

$$\left.\begin{gathered}z_1 \leqslant \tau/\sqrt{1 - q}: \quad \pi_1 = \pi_u(\tau - \sqrt{1 - q}\,z_1), \quad \delta v_{ext_+} = \Phi(\tau - \sqrt{1 - q}\,z_1), \\ \text{with} \quad \pi_u(\tau) \equiv \pi_1|_{z_1=0}, \quad \pi_u(0) = 0, \quad \Phi(\tau) \equiv \delta v_{ext_+}|_{z_1=0}, \quad \Phi(0) = 0\end{gathered}\right\}, \tag{5.7}$$

so that the quasi-uniform pressure in the flame structure is $1 + \varepsilon\pi_u(\tau)$. Using (5.7) in the form $\partial v_{ext_+}/\partial z_1 = -\sqrt{1 - q}\,\partial v_{ext_+}/\partial\tau$, (5.4) yields

$$\frac{\partial v_{ext_+}}{\partial z_1} = \frac{\sqrt{1 - q}}{\gamma}\frac{\partial\pi_1}{\partial z_1} + O(\varepsilon), \tag{5.8}$$

in agreement with the linear relation $\delta p \approx \bar{\rho}\,\bar{a}\,\delta u$ of an acoustic wave propagating from left to right. The flow field $v_{ext_+}(z_1, \tau)$ is obtained by integrating (5.8) from the leading

edge of the compression wave where, to leading order, the boundary conditions (3.19) $v_{ext_+} = S_i + q$ and $\pi_1 = 0$ hold

$$v_{ext_+}(z_1, \tau) - (S_i + q) = \frac{\sqrt{1-q}}{\gamma}\pi_1(z_1, \tau) + O(\varepsilon), \quad \delta v_{ext_+} \approx \frac{\sqrt{1-q}}{\gamma}\pi_1(z_1, \tau). \tag{5.9a,b}$$

According to (5.7) and (5.9*a*,*b*), the relation linking the flow to the pressure just ahead of the flame ($z_1 = 0$) takes the form

$$v_{ext_+}(z_1 = 0, \tau) = S_i + q + \frac{\sqrt{1-q}}{\gamma}\pi_u(\tau) + O(\varepsilon) \tag{5.10}$$

$$\left.\frac{\partial \pi_1}{\partial z_1}\right|_{z_1=0} = -\sqrt{1-q}\frac{\mathrm{d}\pi_u(\tau)}{\mathrm{d}\tau} \Rightarrow \left.\frac{\partial v_{ext_+}}{\partial z_1}\right|_{z_1=0} = -\frac{(1-q)}{\gamma}\frac{\mathrm{d}\pi_u(\tau)}{\mathrm{d}\tau} + O(\varepsilon), \tag{5.11}$$

in agreement with (5.3). These relations are useful for matching the flow of the inner structure with the external flow of unburned gas in § 5.3.

### 5.2. *Matching the temperature*

From now on, the superscript (i) denotes the solution in the preheated zone of the flame structure ($z > 0$). Inside the flame structure, the spatial variation of pressure introduces a negligible term of order $\varepsilon^2$ so that $\partial\pi_1/\partial\tau$ in (4.16) and (4.17) can be replaced by the function $\mathrm{d}\pi_u(\tau)/\mathrm{d}\tau \equiv \partial\pi_1/\partial\tau|_{z_1=0}$ describing the coupling of the flame structure with the external solution on the cold gas. Therefore, (4.16) can be written as

$$z \geqslant 0: \quad \left[\frac{\partial\theta^{(i)}}{\partial\tau} - m(\tau)\frac{\partial\theta^{(i)}}{\partial z} - \frac{\partial^2\theta^{(i)}}{\partial z^2}\right] = \varepsilon\frac{(\gamma-1)}{\gamma}\theta^{(i)}(z, \tau)\frac{\mathrm{d}\pi_u(\tau)}{\mathrm{d}\tau} + O(\varepsilon^2), \tag{5.12}$$

where $\pi_u(\tau) \equiv \pi_1|_{z_1=0}$. The boundary condition at infinity on the cold gas side of the preheated zone ($z = O(1)$, $z \to \infty$) is obtained by matching the preheated zone $\theta^{(i)}(z, \tau)$ and the external flow $\theta_{ext_+}(z_1, \tau)$

$$\lim_{z\to\infty}\theta^{(i)}(z, \tau) = \theta_{ext_+}(z_1, \tau)|_{z_1=0}, \quad \lim_{z\to\infty}\partial\theta^{(i)}/\partial z = \varepsilon\partial\theta_{ext_+}/\partial z_1|_{z_1=0} = O(\varepsilon^2), \tag{5.13a,b}$$

where, according to (5.2) $\theta_{ext_+} = (1-q) + \varepsilon(1-q)[(\gamma-1)/\gamma]\pi_1(z_1, \tau) + O(\varepsilon^2)$, $\partial\theta_{ext_+}/\partial z_1 = O(\varepsilon)$ so that $\lim_{z\to\infty}\partial\theta^{(i)}/\partial z = O(\varepsilon^2)$ is negligible to first order in a perturbation analysis for small $\varepsilon$

$$\lim_{z\to\infty}\theta^{(i)}(z, \tau) - (1-q) \approx \varepsilon(1-q)\frac{\gamma-1}{\gamma}\pi_u(\tau), \quad \lim_{z\to\infty}\partial\theta^{(i)}/\partial z \approx 0. \tag{5.14a,b}$$

Equations (4.13) and (5.12) have to be solved using (5.14*a*,*b*) and the boundary conditions (3.10)–(3.12) on the reaction sheet ($z = 0$) in the distinguished limit (4.9). Equation (3.11) involves the flame temperature $\theta_b(\tau) - 1 \equiv \theta^{(i)}(z, \tau)|_{z=0} - 1 = O(1/\beta)$ which is a time-dependent eigenvalue of the problem, obtained by the jump condition (3.12). In the fully unsteady problem, the solution in the burned-gas side of the reaction sheet $z < 0$ is required in (3.12). We will come back to this question later.

### 5.3. *Matching the flow velocity*

Matching the flow velocity in the preheated zone with the external flow of cold gas yields

$$\lim_{z\to\infty} v^{(i)}(z,\tau) = v_{ext_+}(z_1,\tau)|_{z_1=0} = S_i + q + \frac{\sqrt{1-q}}{\gamma}\pi_u(\tau) + O(\varepsilon), \tag{5.15}$$

$$\lim_{z\to\infty} \frac{\partial v^{(i)}}{\partial z} = \varepsilon \left.\frac{\partial v_{ext_+}}{\partial z_1}\right|_{z_1=0} = -\varepsilon\frac{(1-q)}{\gamma}\frac{\mathrm{d}\pi_u(\tau)}{\mathrm{d}\tau} + O(\varepsilon^2) \tag{5.16}$$

where (5.10) and (5.11) have been used. Equations (5.15) and (5.16) yield

$$\lim_{z\to\infty} v^{(i)}(z,\tau) \to S_i + q + \frac{\sqrt{1-q}}{\gamma}\pi_u(\tau) - \varepsilon z\frac{(1-q)}{\gamma}\frac{\mathrm{d}\pi_u(\tau)}{\mathrm{d}\tau} + O(\varepsilon^2). \tag{5.17}$$

Integration of (4.17), written in the preheated zone in the form

$$\begin{aligned}\frac{\partial v^{(i)}}{\partial z} &= [1-\varepsilon\pi_u(\tau)]\frac{\partial^2\theta^{(i)}}{\partial z^2} - \varepsilon\frac{1}{\gamma}\left[\theta^{(i)} - (1-q)\right]\frac{\mathrm{d}\pi_u(\tau)}{\mathrm{d}\tau} \\ &\quad - \varepsilon(1-q)\frac{1}{\gamma}\frac{\mathrm{d}\pi_u(\tau)}{\mathrm{d}\tau} + O(\varepsilon^2),\end{aligned} \tag{5.18}$$

from the reaction sheet $z=0: v^{(i)} = v_b(\tau)$ yields

$$\left.\begin{aligned} z = O(1): \quad v^{(i)}(z,\tau) - v_b(\tau) &= [1-\varepsilon\pi_u(\tau)]\left(\frac{\partial\theta^{(i)}}{\partial z} - \left.\frac{\partial\theta^{(i)}}{\partial z}\right|_{z=0^+}\right) \\ -\varepsilon\frac{1}{\gamma}\frac{\mathrm{d}\pi_u(\tau)}{\mathrm{d}\tau}\int_0^z\left[\theta^{(i)} - (1-q)\right]\mathrm{d}z &- \varepsilon z(1-q)\frac{1}{\gamma}\frac{\mathrm{d}\pi_u(\tau)}{\mathrm{d}\tau} + O(\varepsilon^2).\end{aligned}\right\} \tag{5.19}$$

Thanks to (5.14*a*,*b*) $\lim_{z\to\infty}\theta^{(i)}(z,\tau) = (1-q) + O(\varepsilon)$, the leading order of the integral on the right-hand side of (5.19) is well defined in the limit $z\to\infty$ and is of order unity. Then, using (5.17), the limit $z\to\infty$ of (5.19) yields

$$\begin{aligned}&v_b(\tau) - \left[S_i + q + \frac{\sqrt{1-q}}{\gamma}\pi_u(\tau)\right] \\ &= [1-\varepsilon\pi_u(\tau)]\left.\frac{\partial\theta^{(i)}}{\partial z}\right|_{z=0^+} + \varepsilon\frac{1}{\gamma}\frac{\mathrm{d}\pi_u(\tau)}{\mathrm{d}\tau}\int_0^{+\infty}[\theta^{(i)} - (1-q)]\,\mathrm{d}z + O(\varepsilon^2),\end{aligned} \tag{5.20}$$

where the thermal flux out of the reaction sheet $\partial\theta^{(i)}/\partial z|_{z=0^+}$ is obtained in terms of the flame temperature $\theta_b$ by the jump condition (3.11). The integral term on the right-hand side of (5.20) is meaningful as soon as $\mathrm{d}\pi_u(\tau)/\mathrm{d}\tau < \varepsilon$.

### 5.4. *Master equation*

Using the jump relation (3.11), (5.20) yields

$$\begin{aligned}&v_b(\tau) - \left[S_i + q + \frac{\sqrt{1-q}}{\gamma}\pi_u(\tau)\right] \\ &= -q\,[1-\varepsilon\pi_u(\tau)]\exp\left[\frac{\beta}{2}(\theta_b - 1)\right] + \varepsilon\frac{1}{\gamma}\frac{\mathrm{d}\pi_u(\tau)}{\mathrm{d}\tau}\int_0^{+\infty}[\theta^{(i)} - (1-q)]\,\mathrm{d}z + O(\varepsilon^2).\end{aligned} \tag{5.21}$$

Anticipating that $\beta(\theta_b - 1)$ is of order unity in the distinguished limit (4.9) and neglecting $\varepsilon$ terms, (5.21) gives a general equation of order unity, called the master equation

$$v_b(\tau) - \left[S_i + q + \frac{\sqrt{1-q}}{\gamma}\pi_u(\tau)\right] = -q\exp\left(\frac{\beta}{2}\left[\theta_b(\tau) - 1\right]\right) + O(\varepsilon). \tag{5.22}$$

This equation is valid for the ZFK model of flames even if the inner structure is unsteady. Under the quasi-steady approximation, (5.22) can be obtained more directly by the conservation of mass across the flame $\bar{U}_b/\bar{U}_L = \bar{T}_b/T_u$ combined with the relation between the laminar flame velocities $\bar{U}_b$ and $\bar{U}_L$ and the flows in the unburned mixture ahead of the flame $u_u$ and in the burned gas $\bar{u}_b$, $u_u - \bar{u}_b = \bar{U}_b - \bar{U}_L = [(\bar{T}_b - T_u)/\bar{T}_b]\bar{U}_b$. The latter expression takes the form $u_u - \bar{u}_b = q\,\bar{U}_b[1 + O(1/\beta)]$ in the limit of large activation energy, the relative variation of the flame temperature $\bar{T}_b(\tau)/\bar{T}_b(0) - 1$ being of order $1/\beta$. Using (5.15) $u_u(\tau) = S_i + q + [\sqrt{1-q}/\gamma]\pi_u(\tau)$ and (2.9) $\bar{U}_b \approx U_b(0)\exp(\beta(\bar{\theta}_b - 1)/2)$, (5.22) is recovered. Although the laminar flame velocity $\bar{U}_b$ (2.9) is no longer valid for an unsteady flame structure, (5.22) is still valid when the unsteady flame temperature $\theta_b(\tau)$ computed from the unsteady flame structure is used on the right-hand side.

## 6. Pressure and flame temperature runaway

In this section the inner structure of the flame is assumed in steady state. The essential mechanism of the pressure runaway is more easily revealed under this approximation. The latter is removed in § 7 leading to the same phenomenology as in § 6.3.

### 6.1. *Quasi-steady inner structure*

If the inner structure of the flame is in steady state (denoted by an overbar), the terms $\partial\theta^{(i)}/\partial\tau$ and $\varepsilon\,\mathrm{d}\pi_u(\tau)/\mathrm{d}\tau$ are neglected in (5.12) leading to

$$\left.\begin{array}{c} z \geqslant 0: \ \bar{Y} = \mathrm{e}^{-\bar{m}z}, \quad \bar{\theta}^{(i)}(z,\tau) = \left[\bar{\theta}_b - \theta_u\right]\mathrm{e}^{-\bar{m}z} + \theta_u, \\ z \leqslant 0: \ \bar{Y} = 1, \quad \bar{\theta}^{(i)} = \bar{\theta}_b(\tau) \end{array}\right\}, \tag{6.1}$$

where the short notation

$$\theta_u(\tau) \equiv (1-q)\left[1 + \varepsilon\frac{\gamma - 1}{\gamma}\pi_u(\tau)\right], \tag{6.2}$$

has been introduced for the gas temperature just ahead of the flame as it is modified by the downstream-running acoustic wave in the unburned gas, see (5.14*a*,*b*). Introducing the parameter $b$ of order unity in the distinguished limit (4.9)

$$b \equiv \frac{\beta\varepsilon}{2}(1-q)\frac{(\gamma-1)}{\gamma}, \quad \varepsilon \to 0, \quad \beta \to \infty: \quad bS_i = O(1), \tag{6.3}$$

the jump conditions acrosss the reaction sheet (3.11) and (3.12) yield

$$\bar{\theta}_b(\tau) = \theta_u + q, \quad \bar{\theta}_b - 1 = \varepsilon(1-q)\frac{\gamma-1}{\gamma}\pi_u + O(\varepsilon^2), \tag{6.4$a$,$b$}$$

$$\beta(\bar{\theta}_b - 1)/2 = \beta\left[\theta_u + q - 1\right]/2 = b\pi_u, \quad \bar{m} = \mathrm{e}^{b\pi_u} + O(1/\beta), \tag{6.5$a$,$b$}$$

$$\bar{\theta}^{(i)}(z,\tau) = q\mathrm{e}^{-\bar{m}z} + (1-q)\left[1 + \varepsilon\frac{\gamma-1}{\gamma}\pi_u(\tau)\right]. \tag{6.6}$$

### 6.2. *Backflow*

In the quasi-steady approximation, the backflow reduces to the instantaneous model (3.16)

$$v_b(\tau) = S\,\bar{m} = S(\tau)\exp(b\pi_u(\tau)). \tag{6.7}$$

Introducing (6.7) into the master equation (5.22) yields the same transcendental equation for the flame pressure $\pi_u = \pi_1|_{z_1=0} = [p/p_{ref}|_{z_1=0} - 1]/\varepsilon = O(1)$ (or the flame temperature) as obtained when the flame is considered as a discontinuity, see Clavin (2022)

$$(S+q)\mathrm{e}^{b\pi_u} = S_i + q + (\sqrt{1-q}/\gamma)\,\pi_u. \tag{6.8}$$

#### 6.2.1. *Turning point*

Introducing the notation

$$\vartheta \equiv b\pi_u = O(1), \quad \zeta \equiv S+q, \quad \zeta(\tau) = (1+\epsilon\tau)S_i + q, \tag{6.9a–c}$$

$$\tilde{b} \equiv b\gamma/\sqrt{1-q} = (\beta\varepsilon/2)(\gamma-1)\sqrt{1-q} = O(1/S_i) \tag{6.10}$$

(6.8) takes the reduced form

$$\zeta\mathrm{e}^{\vartheta} - \zeta_i - \vartheta/\tilde{b} = 0; \quad \tau = 0: \quad \zeta = \zeta_i \equiv S_i + q, \quad \vartheta = 0. \tag{6.11a–c}$$

The solution yields the pressure in terms of the elongation $\vartheta(\zeta)$. The solution depends on the initial elongation $\zeta_i$ and involves a single parameter $\tilde{b}$. Using the elongation vs the time in (3.1) $S(\tau) = [1+\epsilon\tau]S_i$, the solution $\vartheta(\zeta)$ provides us with the dynamics of the pressure and/or the flame temperature. The graph of the inverse function $\zeta(\vartheta)$ is a bell-shaped curve sketched in figure 2, the maximum of which corresponds to $\zeta = \zeta^*$ and $\vartheta = \vartheta^*$

$$\left.\frac{\mathrm{d}\zeta}{\mathrm{d}\vartheta}\right|_{\vartheta=\vartheta^*} = 0: \quad \zeta^*\mathrm{e}^{\vartheta^*} = \frac{1}{\tilde{b}}, \quad \vartheta^* = 1 - \zeta_i\,\tilde{b} > 0, \quad \frac{\zeta^*}{\zeta_i} = \frac{\mathrm{e}^{[\tilde{b}\zeta_i - 1]}}{\tilde{b}\zeta_i} \geqslant 1, \tag{6.12a–c}$$

the inequality $\zeta^*/\zeta_i \geqslant 1$ being valid for all the reactive gaseous mixtures ($0 < \tilde{b}\zeta_i \leqslant 1$), see Clavin (2022). The dynamics of the flame is represented by the C-shaped curve $\vartheta(\zeta)$ with a turning point at the critical elongation $S^*$, $\zeta^* = S^* + q$, $\mathrm{d}\vartheta/\mathrm{d}\zeta|_{\zeta=\zeta^*} = \infty$. There is no more solution to (6.11*a–c*) for $\zeta > \zeta^*$, For $\zeta < \zeta^*$, there are two branches of solutions $\bar{\vartheta}_\pm = \vartheta^* \pm \sqrt{2(\zeta^* - \zeta)/\zeta^*}$, $\bar{\vartheta}_- - \vartheta^* < 0 < \bar{\vartheta}_+ - \vartheta^*$, $\mathrm{d}\bar{\vartheta}_-/\mathrm{d}\zeta > 0$ and $\mathrm{d}\bar{\vartheta}_+/\mathrm{d}\zeta < 0$ for the other, see figure 2. According to the thermodynamics law, the temperature increases during an adiabatic compression so that the physical branch of solutions is $\bar{\vartheta}_-(\zeta)$.

As noticed in Clavin (2022), the limiting case $\zeta_i = \zeta^*$, $S = S^*_{max}$ corresponds to a universal critical Mach number $u^*_u/a^*_u = 2/[\beta(\gamma-1)]$ characterizing the pre-conditioned flow of unburned gas just before the DDT onset. This critical Mach number of the cold flow is typically $u^*_u/a^*_u \approx 0.65$ for ordinary flames ($\beta \approx 8$) and becomes slightly supersonic $u^*_u/a^*_u > 1$ for a very energetic mixture ($\beta \lesssim 4$) while the laminar flame velocity remains very subsonic $U^*_b/a^*_b \approx 0.05$, in agreement with the experiments of Kuznetsov *et al.* (2010) and the numerics of Liberman *et al.* (2010) and Ivanov *et al.* (2011).

#### 6.2.2. *Finite-time singularity of the flow gradient*

According to (6.12*a–c*) $\mathrm{d}\zeta/\mathrm{d}\tau = \epsilon S_i$, the elongation and the flame velocity $\bar{m} = \mathrm{e}^{\vartheta}$ ($\vartheta \equiv b\pi_u$) increase first slowly with the time $\mathrm{d}\bar{m}/\mathrm{d}\tau = O(\epsilon S_i)$, and, according to (6.12*a–c*), the flame acceleration diverges abruptly $\mathrm{d}\vartheta/\mathrm{d}\zeta|_{\zeta=\zeta^*} = \infty$, $\mathrm{d}\bar{m}/\mathrm{d}\tau|_{\tau=\tau^*} =$

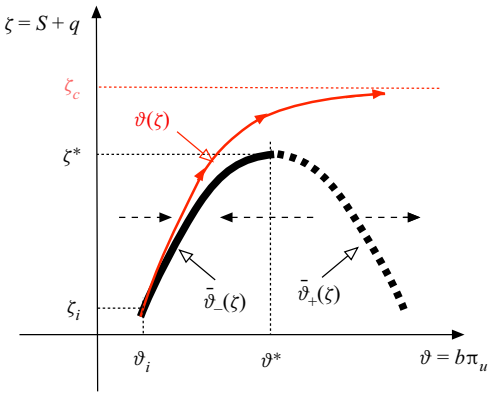


Figure 2. Sketch of the solutions 'elongation $\zeta$ vs pressure $\vartheta$' (not to scale). The two branches $\bar{\vartheta}_\pm(\zeta)$ of solutions of the quasi-steady equation (6.11*a–c*) in thick line show the critical elongation $\zeta^*$, above which no quasi-steady solutions ($\bar{\vartheta}_-$ is the physical solution) exist. The horizontal arrows in broken line indicate the direction of the trajectories of (6.26) for $\tilde{\epsilon}_w > 0$ showing the stability of the branch of physical solutions of (6.11*a–c*), see Strogatz (1994). They are in the opposite direction for $\tilde{\epsilon}_w < 0$. The solution of the dynamical equation (6.26) $\vartheta(\zeta)$ in thin red line shows the finite-time divergence of the pressure at the elongation $\zeta_c > \zeta^*$, $\lim_{(\zeta-\zeta_c)\to 0^-} \vartheta = \infty$. The red arrows indicate the direction of increasing time for an elongation increasing with the time. According to (6.30*a*,*b*), the relative difference in critical elongations is small for a small elongation rate (3.1) $\epsilon \ll 1$: $(\zeta_c - \zeta^*)/\zeta^* = O((\epsilon S_i/\zeta^*)^{2/3})$.

$\epsilon S_i \bar{m}^* \mathrm{d}\vartheta/\mathrm{d}\zeta|_{\zeta=\zeta^*} = \infty$ when the elongation reaches $S^*$, namely when the flame velocity reaches the critical value $\bar{m}^* = \mathrm{e}^{\vartheta^*}$ which is finite ($\vartheta^* < 1$). As in the piston problem considered in Clavin & Tofaili (2021), (6.11*a–c*) takes a generic form near the critical point $\mathrm{d}\zeta/\mathrm{d}\vartheta|_{\vartheta=\vartheta^*} = 0$,

$$\left.\frac{\mathrm{d}^2\zeta}{\mathrm{d}\vartheta^2}\right|_{\vartheta=\vartheta^*} = -\zeta^* \quad \Rightarrow \quad \frac{\zeta^*-\zeta}{\zeta^*} \ll 1 : \frac{\zeta^*-\zeta}{\zeta^*} \approx \frac{1}{2}(\vartheta^*-\vartheta)^2 \tag{6.13}$$

$$\vartheta^* - \vartheta \approx \sqrt{2}\sqrt{\frac{\zeta^*-\zeta}{\zeta^*}}, \quad b(\pi_u^* - \pi_u) \approx \sqrt{\frac{(S^*-S)}{(S^*+q)/2}}, \tag{6.14a,b}$$

obtained by a Taylor expansion. The dynamics of flame pressure and flame temperature near the critical condition at $\tau = \tau^*$ takes the form

$$\vartheta^* - \vartheta(\tau) \approx \kappa\sqrt{\tau^*-\tau} \quad \text{where } \kappa \equiv \sqrt{2\epsilon\frac{S_i}{S^*+q}} = O(\sqrt{\epsilon}), \tag{6.15}$$

exhibiting the finite-time singularity of the flame acceleration

$$\tau/\tau^* - 1 \to 0_- : \ \vartheta \to \vartheta^* = 1 - \zeta_i\tilde{b} > 0, \quad \pi_u \to \pi_u^* = \vartheta^*/b, \quad \bar{m} \to \bar{m}^* = \mathrm{e}^{\vartheta^*} \tag{6.16a–c}$$

$$\frac{\mathrm{d}\vartheta}{\mathrm{d}\tau} \approx \frac{\kappa/2}{\sqrt{\tau^*-\tau}}, \quad \frac{\mathrm{d}\pi_u}{\mathrm{d}\tau} \approx \frac{\kappa/2b}{\sqrt{\tau^*-\tau}}, \quad \frac{1}{\bar{m}}\frac{\mathrm{d}\bar{m}}{\mathrm{d}\tau} \approx \frac{\kappa/2}{\sqrt{\tau^*-\tau}}. \tag{6.17a–c}$$

According to (5.3)–(5.11) and (6.15)–(6.17*a–c*)

$$\left.\begin{aligned} \tau/\tau^* - 1 \to 0_- : \quad \frac{\partial v_{ext_+}(z_1,\tau)}{\partial z_1} &\approx -\frac{(1-q)}{\gamma}\frac{\kappa/2}{b}\frac{1}{\sqrt{\tau^* - \tau + z_1\sqrt{1-q}}}, \\ \frac{\partial v_{ext_+}(z_1,\tau)}{\partial \tau} &\approx \frac{\sqrt{1-q}}{\gamma}\frac{\kappa/2}{b}\frac{1}{\sqrt{\tau^* - \tau + z_1\sqrt{1-q}}}, \end{aligned}\right\} \tag{6.18}$$

the gradient and acceleration of the external unburned flow diverge on the flame

$$\left.\begin{aligned} \tau \to \tau^* : \quad \frac{\partial v_{ext_+}}{\partial z_1}\bigg|_{z_1=0} &\approx \frac{(1-q)}{\gamma}\frac{\kappa/2}{b}\frac{1}{\sqrt{\tau^* - \tau}}, \\ \frac{\partial v_{ext_+}}{\partial \tau}\bigg|_{z_1=0} &\approx \frac{\sqrt{1-q}}{\gamma}\frac{\kappa/2}{b}\frac{1}{\sqrt{\tau^* - \tau}}. \end{aligned}\right\} \tag{6.19$a$,$b$}$$

This suggests a finite-time singularity of the flow gradient leading to the formation of a shock inside the quasi-isobaric flame structure. The DDT mechanism is associated with an even more violent phenomenon: a catastrophic behaviour of the flame structure is predicted below by the delayed backflow model.

### 6.3. *Delayed backflow model. Catastrophic dynamics*

The unsteady flow behind the tip of the elongated flame is a too complex problem for an analytical study. Equation (3.17*a–c*) is a simplified model for studying the main consequence of this unsteadiness, a detailed expression of the delay $\Delta t_w$ is not useful in the following. Only the order of magnitude of $\Delta t_w$ matters for a clear understanding of the phenomenon. Still assuming the inner structure of the flame in steady state $\bar{m} = \mathrm{e}^{b\pi_u(\tau)}$, $\mathrm{d}\bar{m}/\mathrm{d}\tau \approx \bar{m}\, b\, \mathrm{d}\pi_u/\mathrm{d}\tau$ the delayed backflow model (3.17*a–c*) reads

$$v_b = S_i(1+\epsilon\tau)\,\bar{m}\left[1 - \frac{\Delta t_w}{t_{ref}} b \frac{\mathrm{d}\pi_u}{\mathrm{d}\tau} + \dots\right] \tag{6.20}$$

$$v_b \approx S_i \mathrm{e}^{b\pi_u(\tau)} + \epsilon\tau\, S_i \mathrm{e}^{b\pi_u^*} - S_i\, \mathrm{e}^{b\pi_u^*} \frac{\Delta t_w}{t_{ref}} b \frac{\mathrm{d}\pi_u}{\mathrm{d}\tau} + \dots, \tag{6.21}$$

where, considering $\Delta t_w/t_{ref}$ of order unity and $\mathrm{d}\pi_u/\mathrm{d}\tau$ of order $\epsilon < 1$, the $\mathrm{e}^{b\pi_u}$ term in the second and third terms on the right-hand side has been considered as constant nearby the turning point for simplicity.

#### 6.3.1. *Dynamical equation for the pressure and the flame temperature*

Introducing (6.5*a*,*b*) and (6.21) into the master equation (5.22) yields an ordinary differential equation (ODE) of first order for $\pi_u(\tau)$

$$S_i \mathrm{e}^{b\pi_u(\tau)} + \epsilon\tau S_i \mathrm{e}^{b\pi_u^*} - S_i \mathrm{e}^{b\pi_u^*} \frac{\Delta t_w}{t_{ref}} b \frac{\mathrm{d}\pi_u}{\mathrm{d}\tau} - \left[S_i + q + \frac{\sqrt{1-q}}{\gamma}\pi_u(\tau)\right] = -q\mathrm{e}^{b\pi_u(\tau)}, \tag{6.22}$$

which can be written in the form

$$\left[S_i(1+\epsilon\tau) + q\right]\mathrm{e}^{b\pi_u(\tau)} - \left[S_i + q + \frac{\sqrt{1-q}}{\gamma}\pi_u(\tau)\right] = K_w b \frac{\mathrm{d}\pi_u(\tau)}{\mathrm{d}\tau}. \tag{6.23}$$

$$\text{where} \quad K_w \equiv S_i \mathrm{e}^{b\pi_u^*} \frac{\Delta t_w}{t_{ref}} > 0. \tag{6.24}$$

Written with the notation (6.10) and (6.11*a–c*), a nonlinear ODE for $\vartheta(\zeta) = b\pi_u(\zeta)$ is obtained

$$\zeta \exp\vartheta - \zeta_i - \vartheta/\tilde{b} = \tilde{K}_w \frac{\mathrm{d}\vartheta}{\mathrm{d}\zeta}, \quad \text{where } \tilde{K}_w \equiv \epsilon S_i K_w \quad \text{and} \quad \tilde{b} \equiv b\gamma/\sqrt{1-q}. \tag{6.25}$$

The roots of the left hand-side of the first equation (6.25) are the quasi-steady solutions (6.11*a–c*) of the instantaneous backflow model $\overline{\vartheta}_{\pm}(\zeta)$ shown in figure 2. Focusing our attention on the vicinity of the turning point, following (6.15), a power expansion in $(\vartheta - \vartheta^*)$ limited to the quadratic terms yields

$$\frac{(\zeta - \zeta^*)}{\zeta^*} + \frac{(\vartheta^* - \vartheta)^2}{2} = \tilde{\epsilon}_w \frac{\mathrm{d}\vartheta}{\mathrm{d}\zeta}, \quad \text{where } \tilde{\epsilon}_w \equiv \tilde{b}\tilde{K}_w = \epsilon \frac{S_i^2}{\zeta^*} \frac{\Delta t_w}{t_{ref}}. \tag{6.26}$$

For $\zeta < \zeta^*$, the sign of the left-hand side of (6.26) is positive for $\vartheta < \bar{\vartheta}_-$ and for $\vartheta > \bar{\vartheta}_+$ (negative for $\bar{\vartheta}_- < \vartheta < \bar{\vartheta}_+$). The trajectories in the phase space of (6.26) show that the physical branch $\bar{\vartheta}_-(\zeta)$ is stable since $\tilde{\epsilon}_w > 0$. The other branch $\bar{\vartheta}_+(\zeta)$ is unstable. A finite-time singularity of the solution of (6.26) occurs around the turning point, as shown now.

### 6.3.2. *Dynamical saddle-node bifurcation*

Equation (6.26) describes the dynamics nearby a saddle-node bifurcation. Such an equation was extensively used for sharp transitions in different problems of physics or biophysics. The theory of catastrophic events based on this equation has been recently revisited and extended by Peters, Le Berre & Pomeau (2012). Conveniently rescaled

$$(1/2^{2/3})(\zeta^*/\tilde{\epsilon}_w)^{1/3}(\vartheta - \vartheta^*) \to y', \quad (1/2^{1/3})(\zeta^*/\tilde{\epsilon}_w)^{2/3}(\zeta - \zeta^*)/\zeta^* \to t', \tag{6.27a,b}$$

equation (6.26), after multiplication by $(\zeta^*/\sqrt{2}\tilde{\epsilon}_w)^{2/3}$, takes a generic normal form

$$\frac{\mathrm{d}y'(t')}{\mathrm{d}t'} = t' + y'^2, \tag{6.28}$$

with two fixed points for $t' < 0$, the stable one corresponding to the negative root $y' = -\sqrt{-t'}$ (physical branch of solutions). The fixed points collapse at $t' = 0$ and there is no more fixed point for $t' > 0$ (saddle-node bifurcation). Considering an initial condition on the stable branch $t' = t'_i < 0 : y' = -\sqrt{-t'_i}$ for $-t'_i/t'_c = y'^2_i/t'_c$ larger than unity, the asymptotic solution of (6.28) is obtained in terms of the Airy function to give

$$\lim_{t \to t'_c} y'(t') = \frac{1}{t'_c - t'} - \frac{t'_c}{3}(t'_c - t') + \ldots \quad \text{where } t'_c \approx 2.338\ldots; \tag{6.29}$$

see the references in Peters *et al.* (2012). The finite-time singularity (6.29) is of the same type as the solution of the Riccati equation $\mathrm{d}y'/\mathrm{d}t' = y'^2$. According to (6.29), the pressure and the flame temperature $\vartheta \equiv b\pi_u(\tau)$ blow up at time $\tau = \tau_c$ for a finite elongation $\zeta_c = S_i(1 + \epsilon\tau_c) + q$, $(\zeta_c - \zeta^*) = (\tau_c - \tau^*)\epsilon S_i$

$$\frac{\zeta_c - \zeta^*}{(2\zeta^*\tilde{\epsilon}_w^2)^{1/3}} = 2.338\ldots, \quad b(\pi_u - \pi_u^*) \equiv \vartheta - \vartheta^* \approx \frac{2\tilde{\epsilon}}{\zeta_c - \zeta} = \frac{2b\gamma}{\sqrt{1-q}} \frac{K_w}{\tau_c - \tau}. \tag{6.30a,b}$$

The solution to (6.26) increases above the critical elongation $\vartheta(\tau) > \vartheta^*$ and diverges like $K_w/(\tau_c - \tau)$ where $\tau_c - \tau^* \propto K_w^{2/3}/(\epsilon S_i)^{1/3}$, see figure 2. The smaller the elongation

rate $\epsilon < 1$, the closer to the turning point $S^*$ the pressure blowup, $\lim_{\epsilon\to 0}(S_c - S^*)/S_i \propto (\epsilon S_i K_w)^{2/3}$.

To summarize, unsteadiness of the burned-gas flow which is modelled by a delay in the backflow in § 6.3 has a drastic effect on the dynamics, more drastic than the instantaneous backflow in § 6.2: the flame structure is blown off as a whole in finite time when the elongation increases slowly. A strong increase in pressure and flame temperature occurs abruptly with a sudden shrinking of the flame thickness for an elongation slightly larger than the critical elongation of the instantaneous backflow model.

## 7. Unsteadiness of the flame structure

Due to the singularity of the flame acceleration, the quasi-steady approximation of the inner structure of the flame on the tip is doubtful at the end of the process. The objective of this section is to get rid of this assumption.

### 7.1. *Unsteady inner structure of the flame*

Introducing the decomposition $w = \bar{w} + \delta w$ where $\bar{w}$ denotes the quasi-steady approximation of the inner structure, a perturbation analysis of (4.13) and (4.16) is performed in the distinguished limit (4.9)

$$\varepsilon \ll \epsilon \ll 1, \quad \mathrm{d}\pi_u/\mathrm{d}\tau = O(\epsilon), \quad \beta \gg 1, \quad (\gamma-1)\beta\varepsilon S_i = O(1), \tag{7.1a–d}$$

retaining unsteady terms of order $\varepsilon\,\mathrm{d}\pi_u/\mathrm{d}\tau = O(\varepsilon\epsilon)$ in these equation and neglecting smaller terms, namely those of order $\varepsilon(\mathrm{d}\pi_u/\mathrm{d}\tau)^2$ and $\varepsilon^2$. First-order terms are sufficient to draw a final conclusion concerning the finite-time singularity.

#### 7.1.1. *Preheated zone ($z \geqslant 0$)*

Anticipating that $\beta(\theta_b - \bar{\theta}_b) \propto \mathrm{d}\pi_u/\mathrm{d}\tau$ and $\theta^{(i)} - \bar{\theta}^{(i)} \propto \bar{\theta}^{(i)}\,\mathrm{d}\pi_u/\mathrm{d}\tau$, the temperature $\theta^{(i)}$ can be replaced by $\bar{\theta}^{(i)}$ in front of the pressure term on the right-hand side of (5.12)

$$z \geqslant 0: \quad \left[\frac{\partial\theta^{(i)}}{\partial\tau} - m(\tau)\frac{\partial\theta^{(i)}}{\partial z} - \frac{\partial^2\theta^{(i)}}{\partial z^2}\right] \approx \frac{(\gamma-1)}{\gamma}\left[q\mathrm{e}^{-\bar{m}z} + (1-q)\right]\varepsilon\,\frac{\mathrm{d}\pi_u}{\mathrm{d}\tau}, \tag{7.2}$$

$$\lim_{z\to\infty}\theta^{(i)}(z,\tau) = (1-q)\left[1 + \varepsilon\frac{\gamma-1}{\gamma}\pi_u(\tau)\right], \quad \lim_{z\to\infty}\frac{\partial\theta^{(i)}}{\partial z} = 0, \tag{7.3a,b}$$

where the $\varepsilon^2$-terms have been neglected in the boundary conditions (5.14*a*,*b*). Introducing the decomposition

$$\theta^{(i)}(z,\tau) = \bar{\theta}^{(i)} + \delta\theta^{(i)}, \quad m(\tau) = \bar{m} + \delta m, \quad \bar{m} = \mathrm{e}^{b\pi_u}, \tag{7.4a–c}$$

with, according to (6.6),

$$z \geqslant 0: \quad \frac{\partial\bar{\theta}^{(i)}}{\partial\tau} = -qz\mathrm{e}^{-\bar{m}z}\frac{\mathrm{d}\bar{m}}{\mathrm{d}\tau} + \varepsilon(1-q)\frac{(\gamma-1)}{\gamma}\frac{\mathrm{d}\pi_u}{\mathrm{d}\tau}, \quad \frac{1}{\bar{m}}\frac{\mathrm{d}\bar{m}}{\mathrm{d}\tau} = b\frac{\mathrm{d}\pi_u}{\mathrm{d}\tau}, \tag{7.5a,b}$$

equation (7.2) reads after subtracting $\partial\bar\theta^{(i)}/\partial\tau$ and $-\delta m\partial\bar\theta^{(i)}/\partial z = q\bar m\mathrm{e}^{-\bar m z}\delta m$

$$z\geqslant 0:\left[\frac{\partial\delta\theta^{(i)}}{\partial\tau}-\bar m\,\frac{\partial\delta\theta^{(i)}}{\partial z}-\frac{\partial^2\delta\theta^{(i)}}{\partial z^2}\right]\approx -q\,\bar m\,\mathrm{e}^{-\bar m z}\delta m + q\left[b\,\bar m\,z\,\mathrm{e}^{-\bar m z}+\varepsilon\frac{(\gamma-1)}{\gamma}\mathrm{e}^{-\bar m z}\right]\frac{\mathrm{d}\pi_u}{\mathrm{d}\tau}, \tag{7.6}$$

with, according to the boundary conditions (7.3*a*,*b*),

$$\lim_{z\to\infty}\delta\theta^{(i)}=0,\qquad \lim_{z\to\infty}\mathrm{d}\delta\theta^{(i)}/\mathrm{d}z=O(\varepsilon^2). \tag{7.7a,b}$$

Introducing the decomposition $Y=\bar Y+\delta\mathrm{Y}$ into (4.13) using $\bar Y=\mathrm{e}^{-\bar m z}$, $-\delta m\,\partial\bar Y/\partial z=\bar m\mathrm{e}^{-\bar m z}\delta m$ and $\partial\bar Y/\partial\tau=-\bar m\,z\,\mathrm{e}^{-\bar m z}b\,\mathrm{d}\pi_u/\mathrm{d}\tau$ yields

$$\left[\frac{\partial\delta Y}{\partial\tau}-\bar m\,\frac{\partial\delta Y}{\partial z}-\frac{\partial^2\delta Y}{\partial z^2}\right]\approx -\bar m\mathrm{e}^{-\bar m z}\delta m+\bar m\,z\,\mathrm{e}^{-\bar m z}b\,\frac{\mathrm{d}\pi_u}{\mathrm{d}\tau},\qquad \lim_{z\to\infty}\delta Y=0. \tag{7.8a,b}$$

The equation for $\delta Z\equiv\delta\theta^{(i)}-q\delta Y$ is free from the term $\delta m(\tau)$

$$z\geqslant 0:\qquad \left[\frac{\partial\delta Z}{\partial\tau}-\bar m\,\frac{\partial\delta Z}{\partial z}-\frac{\partial^2\delta Z}{\partial z^2}\right]\approx\varepsilon\,q\frac{(\gamma-1)}{\gamma}\mathrm{e}^{-\bar m z}\frac{\mathrm{d}\pi_u}{\mathrm{d}\tau},\qquad \lim_{z\to\infty}\delta Z=0. \tag{7.9a,b}$$

Anticipating that $\delta Z$ is of order $\varepsilon\,\mathrm{d}\pi_u/\mathrm{d}\tau$, neglecting terms of order $\varepsilon\,(\mathrm{d}\pi_u/\mathrm{d}\tau)^2$, the reduced laminar flame speed $\bar m=\mathrm{e}^{b\pi_u}+O(1/\beta)$ is treated as constant in (7.9*a*,*b*). The unsteady term $\partial\delta Z/\partial\tau<\delta Z$ can be neglected in front of $\partial\delta Z/\partial z$ and $\partial^2\delta Z/\partial z^2$ since $\partial/\partial z=O(1)$. After integration $\int_z^\infty\mathrm{d}z$, this yields

$$\left.\begin{aligned} z\geqslant 0:\quad & \bar m\,\delta Z+\frac{\partial\delta Z}{\partial z}=\varepsilon q\frac{(\gamma-1)}{\gamma}\frac{1}{\bar m}\mathrm{e}^{-\bar m z}\frac{\mathrm{d}\pi_u}{\mathrm{d}\tau}\\ \Rightarrow\quad & \bar m\delta\theta_b+\left.\frac{\partial\delta Z}{\partial z}\right|_{z=0^+}=\varepsilon q\frac{(\gamma-1)}{\gamma}\frac{1}{\bar m}\frac{\mathrm{d}\pi_u}{\mathrm{d}\tau},\end{aligned}\right\} \tag{7.10}$$

where the boundary conditions $z=0^+:\ \delta Y=0,\ \delta Z=\delta\theta_b(\tau)\equiv\delta\theta^{(i)}(z=0,\tau)$ have been used. Equation (7.10) can be checked by the small frequency limit of the Fourier transform of (7.9*a*,*b*). Using the relations $\partial\bar\theta^{(i)}/\partial z|_{z=0^-}=0$ and $Y|_{z=0^-}=0$ on the burned-gas side, the jump condition (3.12) takes the form

$$\left.\frac{\partial\theta^{(i)}}{\partial z}\right|_{z=0^-}=\left.\frac{\partial\theta^{(i)}}{\partial z}\right|_{z=0^+}-q\left.\frac{\partial Y}{\partial z}\right|_{z=0^+}\quad\Rightarrow\quad\left.\frac{\partial\delta\theta^{(i)}}{\partial z}\right|_{z=0^-}=\left.\frac{\partial\delta Z}{\partial z}\right|_{z=0^+}. \tag{7.11}$$

According to (7.10) and (7.11), the unsteadiness-induced modification of flame temperature $\delta\theta_b$, $\theta_b=\bar\theta_b+\delta\theta_b$, is expressed in terms of the temperature gradient on the burned-gas side of the reaction sheet

$$\bar m\,\delta\theta_b+\left.\frac{\partial\delta\theta^{(i)}}{\partial z}\right|_{z=0^-}=\varepsilon q\frac{(\gamma-1)}{\gamma}\frac{1}{\bar m}\frac{\mathrm{d}\pi_u}{\mathrm{d}\tau}. \tag{7.12}$$

The right-hand side of (7.12) is part of the perturbation of the flame temperature. The first-order correction to $\beta(\theta_b-1)$ requires the investigation of the temperature in the burned-gas flow ($z<0$) for computing $\partial\delta\theta^{(i)}/\partial z|_{z=0^-}$.

7.1.2. *Burned gas* $z \leqslant 0$

For the analysis of the burned gas, one has to be back to (4.14). According to (6.1) and (6.5*a*,*b*), $\bar{\theta}^{(i)} - 1 = O(\varepsilon\pi_u)$ can be neglected in the factor of the pressure term on the right-hand side of (4.14)

$$z \leqslant 0: \quad \left[\frac{\partial\theta^{(i)}}{\partial\tau} - m(\tau)\frac{\partial\theta^{(i)}}{\partial z} - \frac{\partial^2\theta^{(i)}}{\partial z^2}\right] = \varepsilon\frac{(\gamma-1)}{\gamma}\left[\frac{\partial\pi_1}{\partial\tau} - m(\tau)\frac{\partial\pi_1}{\partial z}\right][1+O(\varepsilon)] \tag{7.13}$$

$$\lim_{z\to-\infty}\theta^{(i)}(z,\tau) = 1, \qquad \lim_{z\to-\infty}\pi_1(z,\tau) = 0, \tag{7.14$a$,$b$}$$

where the boundary conditions (7.14*a*,*b*) at infinity on the burned-gas side are given by the initial condition (hyperbolic problem). Neglecting $\varepsilon\partial^2\pi_1/\partial z^2$ in the burned gas, the energy equation (7.13) and (7.14*a*,*b*) can be written as an entropy equation

$$z \leqslant 0: \left[\frac{\partial}{\partial\tau} - \bar{m}\frac{\partial}{\partial z} - \frac{\partial^2}{\partial z^2}\right]s \approx 0, \quad s \equiv \left[\theta^{(i)} - \frac{(\gamma-1)}{\gamma}\varepsilon\pi_1\right], \quad \lim_{z\to-\infty} s = 1. \tag{7.15$a$–$c$}$$

Anticipating that the unsteadiness-induced disturbances are of order $\varepsilon\,\mathrm{d}\pi_u/\mathrm{d}\tau$, the mass flux $m$ has been replaced by its unperturbed expression $\bar{m}$ on the left-hand side of (7.15*a*–*c*) since the attention is limited to the leading order. Equation (7.15*a*–*c*) shows how the entropy which is generated across the flame structure during the flame acceleration

$$s_b(\tau) \equiv s(z=0,\tau) = \bar{\theta}_b(\tau) + \delta\theta_b(\tau) - (\gamma-1)\varepsilon\pi_u(\tau)/\gamma, \tag{7.16}$$

escapes the reaction zone from the hot side ($m > 0$). This leakage of entropy is the main difference between a flame pushed from behind by a flow of burned gas and an adiabatic (and impermeable) piston. The upstream boundary condition $\lim_{z\to-\infty} s = 1$ can also be viewed as resulting from the damping of the transient variation of entropy by the heat conduction in the (inert) burned gas. The solution to (7.15*a*–*c*) is easily obtained using the Fourier transform $s - 1 = \mathrm{e}^{\mathrm{i}\omega\tau}\tilde{s}_\omega(z)$ and the two relations (6.4*a*,*b*) $\bar{\theta}_b - 1 = \varepsilon(1-q)(\gamma-1)\pi_u/\gamma$ and (7.16), $s_b - 1 = \delta\theta_b - q(\gamma-1)\pi_u/\gamma$

$$z \leqslant 0: \quad \tilde{s}_\omega(z) = \left[\widetilde{\delta\theta_b} - q\frac{\gamma-1}{\gamma}\varepsilon\tilde{\pi}_u\right]\exp\tilde{k}\,z, \tag{7.17}$$

$$\tilde{k}(\omega) \equiv \frac{1}{2}\left[-\bar{m} + \sqrt{\bar{m}^2 + 4\mathrm{i}\omega}\right] \approx \frac{\mathrm{i}\omega}{\bar{m}} + \frac{\omega^2}{\bar{m}^3} + \ldots, \tag{7.18}$$

to give on the reaction sheet, using $\partial\tilde{s}_\omega/\partial z|_{z=0_-} \to \tilde{k}[\widetilde{\delta\theta_b} - q(\gamma-1/\gamma)\varepsilon\tilde{\pi}_u]$ and, in the low frequency limit, $\tilde{k} \to (1/\bar{m})\,\mathrm{d}/\mathrm{d}\tau$

$$\left.\frac{\partial s}{\partial z}\right|_{z=0^-} = \left.\frac{\partial\delta\theta^{(i)}}{\partial z}\right|_{z=0^-} - q\frac{(\gamma-1)}{\gamma}\varepsilon\left.\frac{\partial\pi_1}{\partial z}\right|_{z=0^-} \approx \frac{1}{\bar{m}}\frac{\mathrm{d}\delta\theta_b}{\mathrm{d}\tau} - q\frac{(\gamma-1)}{\gamma}\frac{1}{\bar{m}}\varepsilon\frac{\mathrm{d}\pi_u}{\mathrm{d}\tau}. \tag{7.19}$$

This low frequency result corresponds to the undamped transport by the entropy wave $\partial s/\partial\tau - \bar{m}\partial s/\partial z \approx 0$. The conduction-induced damping rate is of next order in the limit of small frequency. This is similar to freely propagating acoustic waves in planar geometry. In the limit $\varepsilon \ll 1$, the pressure gradient in the burned gas is negligible, the dominant effect being through the increase rate in pressure (time derivative). To avoid any cumulative

effect that could induce acoustical instabilities reviewed in Clavin & Searby (2016), the ends of the tube have been assumed sufficiently far away from the flame. Therefore, neglecting $\varepsilon\partial\pi_1/\partial z|_{z=0^-}$, (7.19) reads

$$\text{burned gas:}\quad \left.\frac{\partial\delta\theta^{(i)}}{\partial z}\right|_{z=0^-} \approx \frac{1}{\bar m}\frac{\mathrm{d}\delta\theta_b}{\mathrm{d}\tau} - q\frac{(\gamma-1)}{\gamma}\frac{1}{\bar m}\varepsilon\frac{\mathrm{d}\pi_u}{\mathrm{d}\tau}. \tag{7.20}$$

7.1.3. *Unsteady modification to the flame temperature*
Introducing (7.20) into (7.12) leads to

$$\bar m\,\delta\theta_b + \frac{1}{\bar m}\frac{\mathrm{d}\delta\theta_b}{\mathrm{d}\tau} \approx 2q\frac{(\gamma-1)}{\gamma}\frac{1}{\bar m}\varepsilon\frac{\mathrm{d}\pi_u}{\mathrm{d}\tau}. \tag{7.21}$$

To first order, the time derivative on the left-hand side of (7.21) is negligible

$$\delta\theta_b \approx 2q\frac{(\gamma-1)}{\gamma}\frac{1}{\bar m^2}\varepsilon\frac{\mathrm{d}\pi_u}{\mathrm{d}\tau} = 2q\frac{(\gamma-1)}{\gamma}\exp[-2b\pi_u]\varepsilon\frac{\mathrm{d}\pi_u}{\mathrm{d}\tau}. \tag{7.22}$$

This can be checked in the low frequency limit of the Fourier transform of (7.21)

$$\widetilde{\delta\theta_b} \approx 2q\frac{(\gamma-1)}{\gamma}\frac{1}{\bar m^2}\frac{\mathrm{i}\omega}{1+\mathrm{i}\omega/\bar m^2}\varepsilon\tilde\pi_u \approx 2q\frac{(\gamma-1)}{\gamma}\frac{1}{\bar m^2}\varepsilon\mathrm{i}\omega\,\tilde\pi_u\left[1-\frac{1}{\bar m^2}\mathrm{i}\omega+O(\omega^2)\right]. \tag{7.23}$$

Thanks to the minus sign in front of $\mathrm{i}\omega$ in the bracket, (7.23) describes a causal response of the flame temperature to the time derivative of pressure. However, the causality link between the flame temperature $\theta_b(\tau)=\bar\theta_b(\tau)+\delta\theta_b(\tau)$ and the pressure $\pi_u(\tau)$ is the reverse

$$\theta_b(\tau) = 1+\varepsilon(1-q)\frac{\gamma-1}{\gamma}\pi_u(\tau) + 2\varepsilon,\, q\frac{(\gamma-1)}{\gamma}\exp[-2b\pi_u]\frac{\mathrm{d}\pi_u}{\mathrm{d}\tau}+O(\varepsilon^2), \tag{7.24}$$

$$\beta(\theta_b-1)/2 = b\left[\pi_u(\tau)+(\Delta\tau_\theta)\,\mathrm{d}\pi_u(\tau)/\mathrm{d}\tau+\dots\right]\approx b\pi_u(\tau+\Delta\tau_\theta), \tag{7.25}$$

$$\left.\begin{aligned}\exp(\beta(\theta_b-1)/2) &\approx \exp(b\pi_u(\tau))\left[1+(\Delta\tau_\theta)b\frac{\mathrm{d}\pi_u(\tau)}{\mathrm{d}\tau}+\dots\right],\\ \Delta\tau_\theta &= \frac{2q}{1-q}\exp(-2b\pi_u)>0,\end{aligned}\right\} \tag{7.26}$$

where, according to (6.3), $b\equiv\beta\varepsilon(1-q)(\gamma-1)/2\gamma=O(1)$ and the $\tau$-variation of $\pi_u$ in the coefficient $\exp(-2b\pi_u)$ in front of $\mathrm{d}\pi_u/\mathrm{d}\tau$ on the right-hand side of (7.24) is negligible since it introduces a correction of following order. Focusing attention near the turning point, the time delay is quasi-constant

$$\Delta\tau_\theta \approx \frac{2q}{1-q}\mathrm{e}^{-2b\pi_u^*} = O(1). \tag{7.27}$$

Equations (7.24)–(7.26) show that the flame temperature and the reaction rate at time $\tau$ are related to the pressure at a later time $\tau+\Delta\tau_\theta$, $\Delta\tau_\theta>0$. As we shall see later, this promotes an instability of the physical branch of the C-shaped curve 'flame velocity vs elongation'.

7.1.4. *Unsteady modification to the mass flux*

Anticipating that $\delta Y$ is of order $\varepsilon\, \mathrm{d}\pi_u/\mathrm{d}\tau \ll 1$, the unsteady term on the left-hand side of (7.8*a*,*b*) can be neglected to first order

$$-\bar{m}\,\frac{\partial \delta Y}{\partial z} - \frac{\partial^2 \delta Y}{\partial z^2} \approx -\bar{m}\mathrm{e}^{-\bar{m}\,z}\delta m + \bar{m}\,z\,\mathrm{e}^{-\bar{m}z} b\,\frac{\mathrm{d}\pi_u}{\mathrm{d}\tau}. \tag{7.28}$$

Integration with the two boundary conditions $z = 0 : \delta Y = 0$ and $\lim_{z\to\infty} \delta Y = 0$ yields

$$\delta Y = -\mathrm{e}^{-\bar{m}z}\, z\delta m + \left[\mathrm{e}^{-\bar{m}z}\frac{z^2}{2} + \frac{1}{\bar{m}}\mathrm{e}^{-\bar{m}z}\, z\right] b\frac{\mathrm{d}\pi_u}{\mathrm{d}\tau}, \tag{7.29}$$

$$\left.\frac{\mathrm{d}\delta Y}{\mathrm{d}z}\right|_{z=0^+} = -\delta m + \frac{1}{\bar{m}} b\,\frac{\mathrm{d}\pi_u}{\mathrm{d}\tau}. \tag{7.30}$$

According to the jump (3.11) and (3.12), the gradients on the flame sheet take the form

$$\left.\frac{\partial \theta^{(i)}}{\partial z}\right|_{z=0^+} = -q\mathrm{e}^{b\pi_u}\left[1 + \frac{\beta}{2}\delta\theta_b + \dots\right], \quad \left.\frac{\partial \delta\theta^{(i)}}{\partial z}\right|_{z=0^+} \approx -q\mathrm{e}^{b\pi_u}\frac{\beta}{2}\delta\theta_b \tag{7.31a,b}$$

$$\left.\frac{\partial \delta\theta^{(i)}}{\partial z}\right|_{z=0^+} = q\left.\frac{\partial \delta Y}{\partial z}\right|_{z=0^+} + O(1/\beta). \tag{7.32}$$

After simplification by $q$, (7.31*a*,*b*) and (7.32) read

$$-\mathrm{e}^{b\pi_u}\frac{\beta}{2}\delta\theta_b = \left.\frac{\partial \delta Y}{\partial z}\right|_{z=0^+} + O(1/\beta). \tag{7.33}$$

Introducing (7.25) into (7.33) and using (7.30) leads to the unsteady modification to the mass flux across the reaction sheet defining the instantaneous laminar flame velocity relative to the burned gas $U_b(\tau)$

$$-\mathrm{e}^{b\pi_u}\Delta\tau_\theta\, b\frac{\mathrm{d}\pi_u}{\mathrm{d}\tau} \approx -\delta m + \frac{1}{\bar{m}} b\,\frac{\mathrm{d}\pi_u}{\mathrm{d}\tau} \quad \Rightarrow \quad \delta m \approx \mathrm{e}^{-b\pi_u}\frac{1+q}{1-q} b\,\frac{\mathrm{d}\pi_u}{\mathrm{d}\tau}. \tag{7.34}$$

The modification of mass flux can be used to compute the variation of the speed of the reaction sheet $U_P(t)$ when the backflow $u_b(t)$ and the flame temperature are known.

## 7.2. *Dynamical effect of the unsteadiness of the inner structure*

The dynamics is governed by the ODE for $\pi_u(\tau)$ when the expressions of $v_b$ and $\beta(\theta_b - 1)$ in terms of $\pi_u$ are introduced into the master equation (5.22). The main difference with the previous analysis of § 6 is that the unsteady flame temperature on the right-hand side of (5.22) is no longer the temperature of the unburned gas simply shifted by the heat release as in a steady laminar flame.

7.2.1. *Instantaneous backflow model*

In a first step, assume for simplicity that the lateral flame (quasi-parallel to the lateral wall) are quasi-steady, the unsteadiness being limited to the flame structure on the tip of the elongated front. Neglecting heat loss at the wall, the temperature in the tongues of unburned gas engulfed near the wall is assumed to be the same as in the flame on the tip of the elongated front, this temperature being modified by the longitudinal compression

wave propagating ahead of the tip. This is an accurate approximation when the elongation is larger than the acoustic wavelength. Then, the instantaneous backflow (3.4) reads

$$v_b(\tau)/S_i = (1+\epsilon\tau)\bar{m}(\tau) = (1+\epsilon\tau)\mathrm{e}^{b\pi_u(\tau)} \approx \mathrm{e}^{b\pi_u(\tau)} + \epsilon\tau\,\mathrm{e}^{b\pi_u^*} + \dots . \tag{7.35}$$

Introducing (7.26) and (7.35) into (5.22) yields

$$S_i\mathrm{e}^{b\pi_u(\tau)} + \epsilon\tau S_i\mathrm{e}^{b\pi_u^*} - \left[S_i + q + \frac{\sqrt{1-q}}{\gamma}\pi_u(\tau)\right] \approx -q\mathrm{e}^{b\pi_u(\tau)} - \mathrm{e}^{-b\pi_u^*}\frac{2q}{1-q}\,b\,\frac{\mathrm{d}\pi_u(\tau)}{\mathrm{d}\tau}, \tag{7.36}$$

which can be written

$$\left[S_i(1+\epsilon\tau)+q\right]\mathrm{e}^{b\pi_u(\tau)} - \left[S_i + q + \frac{\sqrt{1-q}}{\gamma}\pi_u(\tau)\right] = -\mathrm{e}^{-b\pi_u^*}\frac{2q}{1-q}\,b\,\frac{\mathrm{d}\pi_u(\tau)}{\mathrm{d}\tau}, \tag{7.37}$$

and, using the notation (6.10) and (6.11*a–c*),

$$\zeta\,\exp\vartheta - \zeta_i - \vartheta/\tilde{b} = -\tilde{K}_\theta\frac{\mathrm{d}\vartheta}{\mathrm{d}\zeta}, \quad \text{where } \tilde{K}_\theta \equiv \epsilon S_i\,\mathrm{e}^{-b\pi_u^*}\frac{2q}{1-q} > 0 \tag{7.38}$$

$$\frac{(\zeta-\zeta^*)}{\zeta^*} + \frac{(\vartheta^*-\vartheta)^2}{2} = -\tilde{\epsilon}_\theta\frac{\mathrm{d}\vartheta}{\mathrm{d}\zeta}, \quad \text{where } \tilde{\epsilon}_\theta \equiv \tilde{b}\tilde{K}_\theta. \tag{7.39}$$

The difference with (6.25) and (6.26) is the sign on the right-hand side. The negative sign obtained for the instantaneous backflow shows that, according to the trajectories in the phase space of (7.38) and (7.39), the unsteadiness of the inner flame structure promotes an instability of the physical branch $\bar{\vartheta}_-(\zeta)$ of the quasi-steady solutions discussed in § 6.2.1. This would be unfortunate for the study of the DDT when the elongation increases since the physical branch of quasi-steady solutions could not be followed up to the vicinity of the turning point. Hopefully, the delay in the backflow restores the stability as shown now.

### 7.2.2. *Delayed backflow model*

Still assuming that the lateral flames are in steady state, the non-dimensional expression of the delayed backflow is the same as (6.21). Introducing (7.26) and (6.21) into the master equation (5.22) yields a non-dimensional ODE similar to (6.26)

$$\frac{(\zeta-\zeta^*)}{\zeta^*} + \frac{(\vartheta^*-\vartheta)^2}{2} = \tilde{\epsilon}\frac{\mathrm{d}\vartheta}{\mathrm{d}\zeta}, \quad \text{where } \tilde{\epsilon} \equiv \tilde{b}(\tilde{K}_w - \tilde{K}_\theta), \tag{7.40}$$

so that the phenomenology is the same as in § 6.3.2 provided $\tilde{K}_w > \tilde{K}_\theta$ which is typically the case, see the text below (7.43).

### 7.2.3. *Unsteady structure of the lateral flames*

If the inner flame structure of the lateral flames is not in steady state, a delay is involved in the radial flow of burned gas $U_b$ feeding the longitudinal backflow on the axis of the elongated flame front. The unsteady laminar flame velocity $U_b$ of the lateral flames is computed with the first-order disturbance of the mass rate across the reaction sheet $m(\tau)$ in (7.34). The additional delay in the backflow pushing the flame tip takes the form

$$v_b/S_i \approx \mathrm{e}^{b\pi_u(\tau)} + \epsilon\tau\,\mathrm{e}^{b\pi_u^*} + \mathrm{e}^{-b\pi_u^*}\frac{1+q}{1-q}b\frac{\mathrm{d}\pi_u}{\mathrm{d}\tau} + \dots . \tag{7.41}$$

Introducing (7.26) and (7.41) into the master equation (5.22) yields an ODE for $\vartheta = b\pi_u$, namely for the pressure and/or the flame temperature similar to (7.40) but involving an

additional destabilizing term $\tilde{K}_f$

$$\tilde{\epsilon} \equiv \tilde{b}(\tilde{K}_w - \tilde{K}_\theta - \tilde{K}_f), \quad \tilde{K}_f \equiv \epsilon S_i^2 \mathrm{e}^{-b\pi_u} \frac{1+q}{1-q}. \tag{7.42a,b}$$

The same equation as (6.26) is obtained in which $K_w$ is replaced by $K_w - (K_\theta + K_f) > 0$. The same finite-time singularity as that described at the end of § 6.3.2 is obtained, provided the delays satisfy the following condition:

$$\tilde{K}_w > \tilde{K}_\theta + \tilde{K}_f \quad \Rightarrow \quad \frac{L/a_{ref}}{d_{ref}/U_{ref}} > \mathrm{e}^{-2b\pi_u^*} \left[ \frac{1}{S_i} \frac{2q}{1-q} + \frac{1+q}{1-q} \right], \tag{7.43}$$

which is verified for a length of the finger-like flame sufficiently elongated compared to the flame thickness $L/d_{ref} > \mathrm{e}^{-2b\pi_u^*}/\varepsilon$. This is already the case for $\varepsilon \approx 10^{-2}$ and a flame elongation larger than a cell size of a few centimetres (tube diameter).

## 8. Discussion of the results and conclusion

Starting with a small growth rate of elongation from a self-similar solution (quasi-steady solution for a constant elongation), the flame structure is suddenly blown off as a whole in finite time. This occurs for an elongation slightly larger than the critical elongation $S^*$ of the quasi-steady solutions (burned-gas flow and flame structure in steady state). In contrast to the solutions retaining only unsteadiness of the compression waves in the unburned gas, for which the singularity concerns the flow gradients only, a violent increase in pressure and flame temperature develops suddenly while the flame thickness shrinks to zero. The corresponding finite-time singularity is characterized by a dynamical saddle-node bifurcation and develops independently of the precise expression of the delays involved in the unsteady flows provided the condition (7.43) is satisfied.

The finite-time singularity is a consequence of a nonlinear thermal feedback loop between the inner structure of the flame and the compressional heating by the downstream-running compression waves generated in the unburned gas by the accelerating flame acting as a semi-transparent piston. The acceleration is produced by the elongation-induced increase of the self-generated flow. The singularity appears systematically in the vicinity of the turning point whatever the elongation rate, as small as it may be. This is because the flame acceleration of the quasi-steady solution diverges at the turning point. The pre-conditioned state of unburned gas just ahead of the flame and just before the abrupt transition is characterized by a universal critical Mach number of the induced flow of unburned gas which is close to unity, in accordance with the experiments and direct numerical simulations. This critical condition is all the easier to achieve in very energetic mixtures for an elongation which is not much larger than the tube radius. This could well be the case for the cellular structure of Rayleigh–Taylor unstable flame fronts of very energetic mixtures as those involved in supernovae SNIa.

The DDT mechanism is related to the finite-time singularity (6.29) of the solution to (6.28). This equation which is the normal form of a dynamic saddle-node bifurcation has been obtained here by an expansion around the turning point. Therefore, the asymptotic behaviour (6.30*a*,*b*) is not guaranteed for the exact solution of (4.11)–(4.14) satisfying the boundary conditions (3.8)–(3.14). Nevertheless, the onset of a finite-time singularity is not doubtful because unsteady terms of higher order than in (6.28) reinforce the singularity. This is illustrated by the divergence of the acceleration $\mathrm{d}\vartheta/\mathrm{d}\tau \propto 1/\sqrt{\tau^* - \tau}$ in (6.15) becoming $\mathrm{d}\vartheta/\mathrm{d}\tau \propto 1/(\tau_c - \tau)^2$ in (6.29) when unsteadinesses are taken into account. Moreover the singularity is even stronger when unsteady terms of following

order are retained. For example, the divergence is sharper if the term $\mathrm{d}y'/\mathrm{d}t'$ in (6.28) is replaced by a second-order unsteady term $\mathrm{d}^2y'/\mathrm{d}t'^2$ (first Painlevé transcendent), $\mathrm{d}\vartheta/\mathrm{d}\tau \propto 1/(\tau_c - \tau)^3$. The numerical analyses of the one-dimensional problem (2.1*a*,*b*)–(2.4) for the backflow models (3.4)–(3.8) to be published soon by Hernández-Sánchez & Denet confirm the finite-time singularity.

The strong shock generated by the pressure runaway should lead quasi-instantaneously to the DDT. However, molecular dissipation and nonlinearities of the flow are essential in this ultimate phase of DDT. As for the formation of inert shock waves, microscopic length and time scales are involved (mean free path and inverse of the elastic collision frequency). Consequently this ultimate phase cannot be accurately described by macroscopic equations (2.1*a*,*b*)–(2.4). In particular, the maximum shock intensity of the strong overdriven detonation appearing suddenly at the transition requires the Boltzmann equation to be solved. The transverse extension of the explosion should also play a role in that respect. However, once the overdriven detonation is formed, the subsequent relaxation toward the CJ regime (controlled by the rarefaction wave in the burned-gas flow) can be described successfully by the macroscopic equations using the Rankine–Hugoniot jump conditions across the lead shock treated as a discontinuity since the induction length and the thickness of the exothermic reaction zone behind the shock are macroscopic lengths. It is worth stressing once again that the singularity of the flame structure results from the generic divergence of the flame acceleration at the turning point, occurring for any growth rate of elongation (or of flame wrinkling) as small as it may be.

To summarize, the DDT mechanism presented in this article concerns a one-dimensional dynamics of reacting flow characterized by a rate of heat release highly sensitive to the temperature. Although the origin of the self-induced flow is multi-dimensional (increase in surface area of the elongated or wrinkled flame front), the DDT onset is a local process of a one-dimensional nature. This mechanism of transition concerns also turbulent wrinkled flames and/or unconfined cellular flames, the flame brush being considered as a chaotic array of elongated flames the tip of which is accelerated by the self-induced flow associated with the increase in surface area of the flame. In that sense, the DDT mechanism described here could have a certain degree of universality. This should be confirmed by direct numerical simulations keeping in mind the present results.

**Acknowledgements.** Y. Pomeau is acknowledged for enlightening discussions, especially concerning the dynamical saddle-node bifurcation. I am grateful to G. Sivashinsky for drawing my attention few years ago on the work of Joulin and Deshaies. I thank M. Liberman for fruitful discussions on DDT and comments on the manuscript. I thank also Professors B. Denet, G. Lodato, L. Vervisch and the Phd students R. Hernández-Sánchez and H. Tofaili for lively interactions during their numerical activities.

**Funding.** Partial financial support of *Agence National de la Recherche* (contract ANR-18-CE05-0030) is acknowledged.

**Declaration of interests.** The author reports no conflict of interest.

**Author ORCIDs.**
Paul Clavin https://orcid.org/0000-0001-9319-4964.

## References

Binder, C.M. & Orszag, S.A. 1984 *Advanced Mathematical Methods for Scientists and Engineers*. McGraw-Hill International Book Company.

Bykov, V., Koksharov, A., Kuznetsov, M. & Zhukov, V.P. 2022 Hydrogen-oxygen flame acceleration in narrow open ended channels. *Combust. Flame* **238**, 111913.

CLANET, C. & SEARBY, G. 1996 On the tulip flame phenomenon. *Combust. Flame* **105**, 225–238.
CLAVIN, P. 2022 Finite-time singularity associated with the deflagration to detonation transition on the tip of an elongated flame-front in a tube. *Combust. Flame* **245**, 112347.
CLAVIN, P. & CHAMPION, M. 2022 Asymptotic solution of two fundamental problems in gaseous detonations. *Combust. Sci. Technol.* https://doi.org/10.1080/00102202.2022.2041612.
CLAVIN, P. & SEARBY, G. 2016 *Combustion Waves and Fronts in Flows*. Cambridge University Press.
CLAVIN, P. & TOFAILI, H. 2021 Formation of the preheated zone ahead of a propagating flame and the mechanisms underlying the deflagration-to-detonation transition. *Combust. Flame* **232**, 111522.
DESHAIES, B. & JOULIN, G. 1989 Flame-speed sensitivity to temperature changes and the deflagration-to-detonation transition. *Combust. Flame* **77**, 202–212.
HOUIM, W.H., OZGEN, A. & ORAN, E.S. 2016 The role of spontaneous waves in the deflagration-to-detontion transition in submillimetre channels. *Combust. Theor. Model.* **20**( 6), 1068–1087.
IVANOV, M.F., KIVERIN, A.D. & LIBERMAN, M.A. 2011 Hydrogen-oxygen flame acceleration and transition to detonation in a detailed chemical reaction model. *Phys. Rev.* E **83**, 056313.
KAGAN, L. & SIVASHINSKY, G. 2017 Parametric transition from deflagration to detonation: runaway of fast flames. *Proc. Combust. Inst.* **36**, 2709–2715.
KUZNETSOV, M., LIBERMAN, M.A. & MATSUKOV, I. 2010 Experimental study of the preheated zone formation and deflagration to detonation transition. *Combust. Sci. Technol.* **182**, 1628–1644.
LEE, J. 2008 *The Detonation Phenomena*. Cambridge University Press.
LIBERMAN, M.A., IVANOV, M.F., KIVERIN, A.D., KUZNETSOV, M.S., CHUKALOVSKY, A.A. & RAKIMOVA, T.V. 2010 Deflagration-to-detonation transition in highly reactive mixtures. *Acta Astronaut.* **67**, 688–701.
PETERS, D.R., LE BERRE, M. & POMEAU, Y. 2012 Prediction of catastrophes: a experimental model. *Phys. Rev.* E **86**, 026207.
SHCHELKIN, K.I. & TROSHIN, YA.K. 1965 *Gasdynamics of Combustion*. Mono Book Corp.
STROGATZ, S.H. 1994 *Nonlinear Dynamics and Chaos*. Perseus Books Publishing, LLC.
URTIEW, P.A. & OPPENHEIM, A.K 1966 Experimental observations of the transition to detonations in an explosive gas. *Proc. R. Soc. Lond.* A **295**, 13–28.
WU, M., BURKE, M.P., SON, S.F. & YETTER, R.A. 2007 Flame acceleration and the transition to detonation of stoichiometric ethylene/oxygen in microscale tubes. *Proc. Combust. Inst.* **31**, 2429–2436.
WU, M. & WANG, C. 2011 Reaction propagation modes in millimeter-scale tubes for ethylene/oxygen mixtures. *Proc. Combust. Inst.* **33**, 2287–2293.
ZELDOVICH, YA.B. 1980 Regime classification of an exothermic reaction with nonuniform initial conditions. *Combust. Flame* **39**, 211–214.